APPLICATION OF ENSEMBLE-BASED OPTIMIZATION ON UNISIM-I

A Thesis

by

PATTANAPONG PLUKMONTON

Submitted to the Office of Graduate and Professional Studies of
Texas A&M University
in partial fulfillment of the requirements for the degree of

MASTER OF SCIENCE

Chair of Committee,	Eduardo Gildin
Committee Members,	Hadi Nasrabadi
	Zenon Medina-Cetina
Head of Department,	A. Daniel Hill

May 2017

Major Subject: Petroleum Engineering

ABSTRACT

In reservoir management, it is challenging to obtain an efficient production schedule and maximize the profits. An optimization workflow is usually used in maximizing/minimizing the production objective. However, production optimization is not an easy task and could be time-consuming since the reservoir and the production optimization itself consist of complex subsystems and uncertainties. Thus, many studies have been done to propose optimization methods that are efficient and yet practical in finding the optimal strategy. Most of these methods usually focus on the gradient-based approaches, where the information from gradients of the objective function with respect to control parameters is used in finding the optimal solutions.

One of the gradient-based methods that recently has gained popularity in petroleum production optimization is Ensemble-based Optimization (EnOpt). In EnOpt, the gradient is approximated using a linear regression between an ensemble of control vectors and their corresponding objective function values. Thus, the computational cost of the method relies on the number of realizations in the control ensemble and is nearly independent of the number of control parameters. Moreover, the EnOpt can be used with any reservoir simulator without modification to the simulator. Many publications have demonstrated that EnOpt gave a good optimized-result on different reservoir models and recovery techniques.

In this thesis, we study the benefits of the EnOpt applied to waterflooding optimization problems using realistic reservoir data. In particular, the EnOpt is used to optimize the waterflooding process in a benchmark reservoir, namely UNISIM-I. The objective of this optimization is to maximize the expected net present value (NPV) over 20 years of production. The control parameters are injection and production rates in injector and producer wells. We consider two optimization problems: random initial control settings and extended production from the production history. The EnOpt was successful in finding optimal solutions in both cases with significantly cheaper computational cost required in gradient calculations. In addition, we study the effect of discount rate use in calculating the NPV: the short-term EnOpt uses high discount rate, whereas the long-term EnOpt sets discount rate equal to zero. The different discount rates result in different optimal solutions. The high discount rate results in an increase of cash flow in the early stages of the production time while low to no discount rate results in an increase of cumulative cash flow throughout the production time.

ACKNOWLEDGEMENTS

I would like to thank my committee chair, Dr. Euardo Gildin, and my committee members, Dr. Hadi Nasrabadi and Dr. Zenon Medina-Cetina, for their guidance and support throughout the course of this research.

Thanks also go to my friends and colleagues, the department faculty and staff for making my time at Texas A&M University a great experience.

Thanks to my mother and father for their encouragement and to my girlfriend for her patience and love.

CONTRIBUTORS AND FUNDING SOURCES

Contributors

This work was supervised by a thesis committee consisting of Dr. Eduardo Gildin and Hadi Nasrabadi of the Harold Vance Department of Petroleum Engineering, and Dr. Zenon Medina-Cetina of the Zachry Department of Civil Engineering.

All work for the thesis was completed independently by the student.

Funding Sources

Graduate study was supported by a full scholarship from the Department of Mineral Fuels, Ministry of Energy of Thailand.

The contents in this thesis are solely the responsibility of the author and do not necessarily represent the official views of the Department of Mineral Fuels.

TABLE OF CONTENTS

Page

LIST OF FIGURES

Page

Page

LIST OF TABLES

Page

1. INTRODUCTION

Reservoir production optimization has always played a significant role in petroleum field developments as it seeks for an optimal control strategies that increases recovery of the petroleum in place. In the initial state of the production, the main driving force is the reservoir pressure. But, as oil is being produced from the reservoir, the reservoir pressure decreases. Therefore, processes called secondary recoveries are performed to maintain the reservoir pressure and to increase the oil recovery. Although many secondary recovery methods can be used together with the production optimization to improve petroleum recovery, the thesis focuses on a waterflooding process, a commonly used secondary recovery method.

Optimization methods usually requires the use of reservoir simulation models to evaluate future production in order to select the new control strategy. Thus, this framework is sometimes called "Model-based production optimization". However, the reservoir simulation is a time-consuming task due to the complexity of the reservoir model, and thus many optimization methods have been developed to reduce the model simulation requirements, while maintaining the accuracy in computing the optimal solution. The optimization techniques can be categorized into two classes: Stochastic algorithms, such as Genetic Algorithm and Simulated Annealing; and gradient-based algorithms, such as steepest ascent and quasi-Newton. Since the stochastics approaches rely on randomization principle, they usually find the optimal solution with a sufficiently large number of simulation runs. This makes stochastic approaches not practical for petroleum production

optimization. The gradient-based approaches, on the other hand, use the information from the gradient of the objective function with respect to control parameters to seek for an optimal solution. Hence, the approaches reach the optimal solution with fewer simulation runs.

In this thesis, we focus on the production optimization using gradient-based approaches. Various methods have been developed to compute the gradient including numerical perturbation, adjoint method, and ensemble-based method. The numerical perturbation method (finite difference approximation) is very easy to implement. The gradient is computed by perturbing each control parameter and running the simulator to determine a perturbed objective function. Therefore, the number of simulation runs required is proportional to the number of control parameters. Since the production optimization problem usually consists of a large number of control parameters, the numerical perturbation method becomes extremely time consuming and not practical to use for gradient computation in our optimization scheme.

The most efficient method in term of a computational requirement is the adjoint method. The method computes gradient using one forward simulation and one backward, or adjoint simulation, regardless of the size of a control vector. The method has been shown to work very well in production optimization (Brouwer et al. 2004, Sarma et al. 2005). Unfortunately, implementing the adjoint method requires a modification to a reservoir simulator code, which is a time consuming and code-intrusive task.

Alternatively, many methods that are non-intrusive to the simulator code have been developed. One of these methods that has gained popularity in petroleum production

optimization scheme is an Ensemble-based Optimization (EnOpt) proposed by Chen (2008). The method computes an approximate gradient using the sensitivity that is provided by the ensemble of control vectors and their corresponding objective function values. The concept of generating an approximate gradient from an ensemble of control vectors in optimization problem is actually originated by Lorentzen et al. (2006), followed by (Wang et al. 2007). The idea of the gradient approximation in these studies are based on the method called ensemble Kalman filter method (EnKF) used in data assimilation. However, the name EnOpt was proposed by Chen (2008). Do et al. (2013) make an analysis of the EnOpt and shows that the method is similar to other stochastic gradient estimation methods such as simultaneous perturbation stochastic approximation (SPSA) and the simplex gradient method (Conn et al. 2009). The method gives the flexibility to use different reservoir simulators and solution methods. The computational cost is nearly independent of the size of control parameters. Moreover, the quality of the gradient approximation depends on the number of realizations in the ensemble and the level of nonlinearity of the problem. Many studies (Chaurdhri et al. 2009, Chen et al. 2009, Fonseca et al. 2014, Leeuwenburgh et al. 2010) have shown that the ensemble-based method has worked very well in the production optimization problems. Also, many recent studies purpose a modified EnOpt formulation to achieve better optimization result (Chaurdhri et al. 2009, Fonseca et al. 2013, Fonseca et al. 2014, Fonseca et al. 2017).

1.1 Objective

In order to test the EnOpt to a realistic production optimization case, in this thesis, we study the standard EnOpt proposed by Chen (2008) and apply the method to a large production scale in a synthetic reservoir namely UNISIM-I. The UNISIM-I is designed to be a comparative case for reservoir management, based on a real formation structure in Namorado oil field, located in Campos Basin, Brazil. Since it is shown that there was no previous study has used the EnOpt to optimize the production of the UNISIM-I, our goal is to study the benefits of the EnOpt on the production of the reservoir. The optimization objective is to maximize an expected net present value by adjusting injection and production rates in the injectors and producers. The production period for optimization is 20 years with 1-year control steps. Moreover, we study an effect of a discount rate, a parameter in the net present value function, on the optimal solution. Two optimization cases with different discount rate are performed and the discussion is made on their results.

There are five sections in the thesis. Section 2 briefly lay out the related background theories for production optimization. It discusses the production optimization, algorithm and the use of reservoir simulation. Section 3 discusses the EnOpt, as a gradient approximation method used with steepest ascent algorithm. Two illustrative examples are shown capturing the performance of EnOpt. Section 4 illustrates the application of the EnOpt on the UNISIM-I and the discussion on the results. Section 5 summarizes the principal conclusions from this study and discusses on future improvement for this study.

2. BACKGROUND THEORY

2.1 Introduction of Reservoir Simulation

The petroleum production optimization that is studied in this thesis can also be referred as a model-based production optimization. The term *model* refers to a reservoir simulation model, a type of porous media flow simulator that is used to simulate a flow profile of the liquid in the formation of a reservoir of interested. The reservoir simulation model consists of two types of sub-models, fluid flow model, and geological model. The fluid flow model is a mathematical model that describes how fluids flow in a porous medium. The geological model describes the rock formation, the reservoir. It gives information on the petrophysical properties as well as the geometry of the reservoir. In this section, we only discuss some basic idea of reservoir simulation. The detail of reservoir simulation can be found in Aziz et al. (1979), Chen et al. (2006), and Ertekin et al. (2001).

The reservoir simulation model used in our studies is set up under the following assumptions: incompressible rock, and immiscible and incompressible fluids. In addition, the fluid system is composed of two phases: water - wetting phase, which is indicated by a subscript w, and oil – nonwetting phase indicated by o. To develop a generic system of flow equations for two-phase flow, we use the fundamental principle of mass conservation. For a system of 2 immiscible fluid phases, the conservation equation for each phase can be written as

$$\frac{\delta}{\delta t}(\phi S_\alpha \rho_\alpha) = -\nabla \bullet (\rho_\alpha \boldsymbol{u}_\alpha) + q_\alpha \qquad \alpha = o, w \tag{1}$$

where ϕ is the porosity of the porous medium; S_α denotes saturation or fraction of the pore volume occupied by phase α; ρ_α, $\boldsymbol{u}_\alpha$, and q_α are density, Darcy's velocity, and mass flow rate of the phase α, respectively.

The Darcy's law, used in single phase flow, can be extended to multiphase flow as follow

$$\boldsymbol{u}_\alpha = -\frac{k_{r\alpha}}{\mu_\alpha}\boldsymbol{k}(\nabla p_\alpha - g\rho_\alpha \nabla z) \quad \alpha = o, w \tag{2}$$

where $\boldsymbol{k}$ is the absolute permeability; $k_{r\alpha}$, p_α, and μ_α are the relative permeability, pressure, and viscosity of the phase α, respectively; g is gravitational acceleration; z is the vertical depth. For two-phase fluid system, the pore-volume is occupied by either oil or water. Hence, the relationship of the saturation of each phase is

$$S_o + S_w = 1 \tag{3}$$

Because of the surface tension, the equilibrium pressure in each phase will be different. The pressure difference between the two phases is given by the capillary pressure p_c, which is a function of water saturation S_w,

$$p_c(S_w) = p_o - p_w \tag{4}$$

Now, we use (3) and (4) and combine variables to only oil pressure p_o and water saturation S_w as the primary variables:

$$p = p_o, S = S_w \tag{5}$$

Also, we define the total velocity,

$$\boldsymbol{u} = \boldsymbol{u_w} + \boldsymbol{u_o} \tag{6}$$

Under the assumption that the fluids are incompressible, we get

$$\nabla \bullet \boldsymbol{u} = \tilde{q}(p, S) \equiv \tilde{q}_w(p, S) + \tilde{q}_o(p, S) \tag{7}$$

$$\boldsymbol{u} = -\boldsymbol{k}\left[\lambda(S)\nabla p - \lambda_w(S)\nabla p_c - (\lambda_w \rho_w + \lambda_o \rho_o) g \nabla z\right] \tag{8}$$

where $\tilde{q}_w = \frac{q_w}{\rho_w}$ and $\tilde{q}_o = \frac{q_o}{\rho_o}$, and the phase mobility λ_α and total mobility λ are defined as

$$\lambda_\alpha(S_\alpha) = \frac{k_{r\alpha}(S_\alpha)}{\mu_\alpha} \qquad \alpha = w, o \tag{9}$$

$$\lambda(S_w) = \lambda_w(S_w) + \lambda_o(1 - S_w) \tag{10}$$

Combine (7) and (8), yields the *pressure equation*,

$$-\nabla \bullet (\boldsymbol{k}\lambda \nabla p) = \tilde{q} - \nabla \bullet \left(\boldsymbol{k}(\lambda_w \nabla p_c + (\lambda_w \rho_w + \lambda_o \rho_o) g \nabla z)\right) \tag{11}$$

Similarly, we apply (4), (6), and (8) into (1), (2) with $\alpha = w$ to obtain the *saturation equation*.

$$\phi \frac{\delta S}{\delta t} = \tilde{q}_w(p, S) - \nabla \bullet \left(\boldsymbol{k} f_w(S) \lambda_o(S) \left(\frac{dp_c}{dS} \nabla S + (\rho_o - \rho_w) g \nabla z\right) + f_w(S)\boldsymbol{u}\right) \tag{12}$$

where the fractional flow f_α is

$$f_\alpha = \frac{\lambda_\alpha}{\lambda} \tag{13}$$

Here, we solve (11), (12) for pressure and saturation using the *implicit pressure, explicit saturation* method (IMPES). To solve for pressure, it is assumed that p, $\boldsymbol{u}$, and S are known at time t and that we evolve the solution to time $t + \Delta t$. At the beginning of time step, we fix the saturation S and solve for p implicitly using (11). Then we use the updated $\boldsymbol{u}$ to solve for and updated saturation S at next time step using (12). Here, we discretize the left-hand side of (12) into time step Δt_i,

$$\phi \frac{\delta S}{\delta t} \approx \phi \frac{S^{n+1} - S^n}{\Delta t^{n+1}} \tag{14}$$

We use the MATLAB Reservoir Simulation Toolbox (MRST) as the reservoir simulator. The toolbox provides varieties of functions that can be used for gridding, discretization, and a solver for flow and transport in different kinds of reservoirs. Lie et al. (2012), and Lie (2016) give details of the available functions in MRST and how to set up the reservoir simulation model.

2.2 Production Optimization

The production optimization is a workflow that seeks for a new operating strategy that maximizes/minimizes the production objective. Mathematically speaking, production optimization problem can be written as

$$\begin{aligned} &\max_{\boldsymbol{x}\in R^n}/\min\, g(\boldsymbol{x}) \\ &\text{subject to } \begin{cases} c_i(x) = 0 & i \in \varepsilon \\ c_i(x) \geq 0 & i \in \zeta \end{cases} \end{aligned} \tag{15}$$

where $g(\boldsymbol{x})$ denotes the objective function to be optimized, c_i where $i \in \varepsilon$ are the equality constraints, and c_i where $i \in \zeta$ are the inequality constraints. In the scope of petroleum production optimization, the objective function can be from an expected net present value (NPV), the ultimate recovery (UR) of the reservoir, or other quantities depending on financial goals. The control parameters used in the optimization problem is denotes by the vector $\boldsymbol{x}$ where

$$\boldsymbol{x} = \left[x_1, x_2, \dots, x_{N_x}\right] \tag{16}$$

The vector of control parameters contains all the optimization constraints in all control steps. For the petroleum production, theses parameters can be, for example, water injection rate, liquid production rate, bottom hole pressure of injector or producer, etc. In addition,

we use N_x to denote the total number of control parameters, which equals to the product of control parameters at each time steps and the number of control steps. For example, an optimization problem that optimizes the cumulative oil production through injection and production rate of a total of 20 wells with 30 control time steps would have the total number of control parameters $N_x = 600$.

Several optimization methods have been developed, such as genetic algorithm and simulated annealing, steepest ascent, conjugate gradient, and quasi-Newton. These optimization methods can be categorized into stochastic- and gradient-based approaches. The stochastics approaches rely on randomization principle. In each iteration, several control vectors are randomly sampled, and being evaluated using a reservoir simulator to determine the optimal solution. Thus, the stochastic optimization approaches require a sufficiently large number of simulation runs. Since the reservoir model is usually a very complex model, running each reservoir simulation is a time-consuming task. This makes stochastic approaches not practical for petroleum production optimization due to its computational requirement. The gradient-based approaches, on the other hand, seek for an optimal solution using the information from the gradient of the objective function with respect to control parameters. The approaches usually reach the optimal solution with fewer simulation runs. Hence, to reduce computational cost from a reservoir simulation, this thesis focuses only on the gradient-based approaches for the production optimization.

2.3 Gradient-based Production Optimization

The gradient-based optimization methods refer to the optimization methods that require computations of the gradient ∇g of an objective function $g(\boldsymbol{x})$ with respect to the control parameters $\boldsymbol{x}$ to determine a search direction for optimal solution,

$$\nabla g = \left[\frac{\delta g}{\delta x_1}, \frac{\delta g}{\delta x_2}, \ldots, \frac{\delta g}{\delta x_{N_x}}\right] \tag{17}$$

Since a production optimization problem is usually a complex interplay of several subsystems, computing the gradient analytically, like in (17), is not possible. Therefore, several numerical gradient calculation methods have been proposed. One of the simplest ways to compute the gradient is by using numerical perturbation method. The gradient is numerically calculated as follow

$$\frac{\delta g}{\delta x_i} \approx \frac{g(x_i + dx_i) - g(x_i)}{dx_i} \text{ for } i = 1, 2, \ldots, N_x \tag{18}$$

From (18), the gradient is computed by perturbing each control parameter $x_i + dx_i$ and running the simulator to determine a perturbed objective function $g(x_i + dx_i)$. Thus, the number of simulation runs required to obtain a gradient is proportional to the number of control parameters. The major drawback of this method relies on the fact that the reservoir model is a complex system and running the model simulation is time-consuming. Wang et al. (2007) used the perturbation method to compute the gradient and concluded that since the optimization problem consists with a large number of control parameters and each perturbation requires one simulation run, the method is very time-consuming and not practical for the production optimization problem.

The adjoint method (Brouwer et al. 2004, Sarma et al. 2005) can significantly reduce the computational requirement for computing gradient. The method requires one forward simulation, and one backward simulation (fully implicit simulator) regardless of the size of control parameters $\boldsymbol{x}$ to compute the gradient. Although this method is very efficient, its drawbacks are that the method is intrusive to the simulator code since it requires access to the simulator source code to get an implicit simulation (Sarma et al. 2005). Moreover, when the optimization problem consists of a very large number of control parameters, the adjoint method becomes very expensive due to its massive storage requirements (Chen et al. 2009). Also, calculating gradient using the adjoint method can result in gradients that lead to local minima since the method results in a linearization about the current model (Chen 2008).

Wang et al. (2007) used a modified ensemble Kalman filter (EnKF), a data assimilation method, in a production optimization. The modified EnKF successfully optimized the problem although it gives a poor estimate of the optimal solution. Chen (2008) proposed an ensemble-based production optimization (EnOpt) based on the same idea. The optimization uses the steepest ascent method to update the control parameters where the gradient is approximated by the sensitivity of an ensemble of control samples and their corresponding objective function values. Chen (2008) demonstrated the proposed optimization approach on a synthetic reservoir with known properties. The result showed a significant increase in the NPV of the reservoir compared to the reference case.

The EnOpt have advantages over both numerical perturbation method and adjoint method. Unlike numerical perturbation method, EnOpt approximates the gradient with

nearly independent of the number of control parameters. The quality of the gradient approximation depends on the size of the ensemble and the level of nonlinearity of the problem (Chen 2008, Fonseca et al. 2015). In addition, the EnOpt does not require a modification to a reservoir simulator. Thus, the method can be used with most commercial simulators. With these advantages in mind, the EnOpt seems to be a good method for gradient calculation when using gradient-based optimization.

This thesis studies Chen's (2008) EnOpt. The production optimizations are performed using steepest ascent method with the gradient approximated by EnOpt. The following section discusses steepest ascent method, and in Section 3, we discuss the detail of the gradient approximation using EnOpt.

2.4 Steepest Ascent Method

One of the simplest and well-known gradient-based methods for maximizing or minimizing a function is the steepest ascent method (Cauchy 1847, Meza 2010).

Suppose that we would like to maximize an objective function $g(\boldsymbol{x})$ where $x \in \boldsymbol{R}^n$ and that $g: \boldsymbol{R}^n \rightarrow \boldsymbol{R}$. The idea of this maximization method is to find an iterate control vector $\boldsymbol{x}^{k+1}$ along search direction $\boldsymbol{p}^{\boldsymbol{k}}$, with step size α^k away from the current control vector $\boldsymbol{x}^k$,such that $g\left(\boldsymbol{x}^{k+1}\right) > g\left(\boldsymbol{x}^k\right)$

$$\boldsymbol{x}^{k+1} = \boldsymbol{x}^k + \alpha^k \boldsymbol{p}^k \quad \text{where } k = 0, 1, \ldots \tag{19}$$

For steepest ascent method, the search direction $\boldsymbol{p}^k$ is defined by a gradient ∇g^k of the function g evaluated at $\boldsymbol{x}^k$,

$$\boldsymbol{p}^k = \nabla g^k \tag{20}$$

In this thesis, the gradient ∇g^k is approximated using a so-called *ensemble-based method*. The detail of the gradient approximation using ensemble-based method will be discussed later in Section 3. In addition, to determine a step size α^k, we use the backtracking line search algorithm with sufficient increase condition (Nocedal et al. 2006), which will be discussed in the following sections.

2.4.1 Line search algorithm

From equation (19), at each iteration, we need to choose the step size α^k such that it gives a substantial increase in the function g. In another word, we want to find the step size α^k along the search direction $\boldsymbol{p}^k$ such that it maximize the univariate function $\phi(\bullet)$ defined by

$$\phi(\alpha) = g\left(\boldsymbol{x}^k + \alpha \boldsymbol{p}^k\right), \qquad \alpha > 0 \tag{21}$$

However, to identify an exact value of α^k requires too many evaluations of the objective function g and its gradient ∇g. Instead, an inexact line search is performed to determine a step size α^k that achieves an increase in g at minimal cost (Nocedal et al. 2006).

We now discuss a popular inexact line search condition stipulates that α^k should give *sufficient increase* in the objective function g, as measured by the following inequalities:

$$\begin{aligned} g\left(\boldsymbol{x}^k + \alpha \boldsymbol{p}^k\right) &\geq g\left(\boldsymbol{x}^k\right) + c\alpha\left(\nabla g^k\right)^T \boldsymbol{p}^k \\ \phi(\alpha) &\geq l(\alpha) \end{aligned} \tag{22}$$

The function $l(\bullet)$ has a positive slope $c\left(\nabla g^k\right)^T \boldsymbol{p}^k$, where $c \in (0,1)$. Thus, for a small positive value of α, the graph of l lies below the graph of ϕ (see Figure 1). The sufficient increase condition accepts α only if $\phi(\alpha) \geq l(\alpha)$. Note that the value of c is chosen to be very small, 10^{-4} for our cases.

Nocedal et al. (2006) point out that the sufficient increase condition (22) alone is not enough to ensure that the algorithm makes reasonable progress along the given search direction. Unless we use a so-called *backtracking method*, the second condition is required to rule out unacceptable short steps. Therefore, we choose to implement backtracking method with the sufficient increase condition to ensure that the step size is appropriately chosen. The algorithm of the backtracking method is shown in Figure 2.

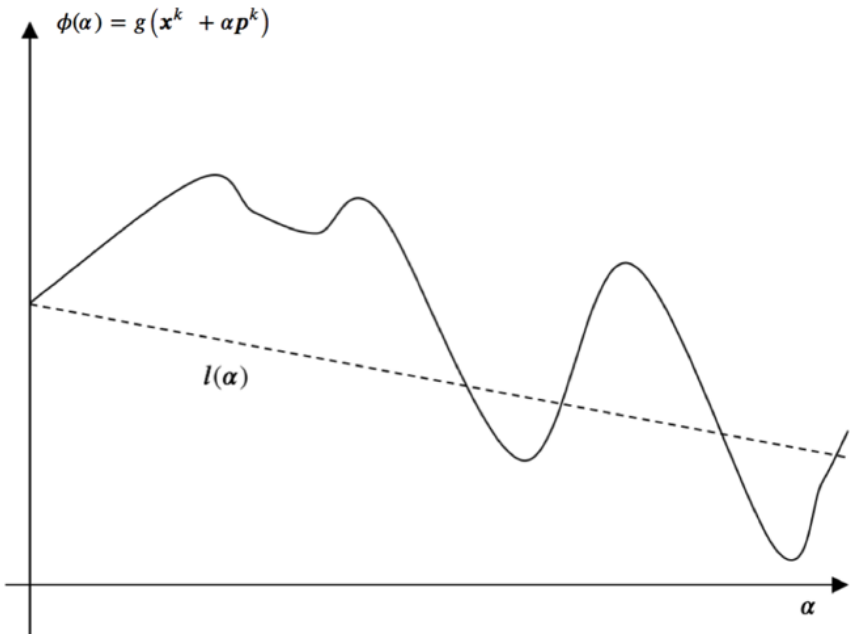

Figure 1: Sufficient increase condition (Modified from Nocedal et al. (2006)).

Backtracking Line Search Algorithm

Set $\bar{\alpha} > 0$, $\rho \in (0,1)$

START

1) $\alpha = \bar{\alpha}$
2) Check if $g\left(\boldsymbol{x}^k + \alpha \boldsymbol{p}^k\right) \geq g\left(\boldsymbol{x}^k\right) + c\alpha\left(\nabla g^k\right)^T \boldsymbol{p}^k$

YES: Terminate with $\alpha^k = \alpha$

NO: Replace α with $\rho\alpha$

END

Figure 2: Backtracking line search algorithm (Modified from Nocedal et al. (2006)).

During line search, the new step size $\alpha' = \rho\alpha$ is chosen within the previous trial value of α, which was rejected for violating the sufficient increase condition. In another word, the previous trial step size was too long. Thus, the backtracking method ensures the selected step size α_k is short enough to satisfy the sufficient increase condition but not too short. Moreover, with backtracking method, an acceptable step size will be found after a finite number of trials since the step size α will eventually become small enough that the sufficient increase condition in (22) is satisfied.

2.4.2 Initial step size

In the case when using Newton or quasi-Newton methods for optimization, we can always use the initial step size $\alpha_0^k = 1$. However, for the steepest ascent method, it does not produce well-scaled search direction. Therefore, it is important to use current information about the problem and the algorithm to make the initial guess for the step size (Nocedal et al. 2006). In each iteration, an initial step size α_0^k is determined under an

assumption that the first-order change in the function at iterate $\boldsymbol{x}^k$ will be the same as the previous iteration, that is

$$\alpha_0^k = \alpha^{k-1} \frac{(\nabla g^{k-1})^T \boldsymbol{p}^{k-1}}{(\nabla g^k)^T \boldsymbol{p}^k} \qquad k = 2, 3, \ldots \tag{23}$$

At this point, we have discussed basic concepts used in production optimization. The remaining thing to do now is to determine a search direction p^k in the steepest ascent method, or the gradient ∇g of the objective function with respect to the control parameters. In the following section, we will introduce the use of the ensemble method to approximate the gradient ∇g used in steepest ascent for production optimization.

3. ENSEMBLE-BASED OPTIMIZATION (EnOpt)

In this section, the main theory of the ensemble-based optimization (EnOpt) using steepest ascent method will be briefly discussed based on the original EnOpt by Chen (2008). For an in-depth discussion, the reader is referred to Chen (2008). The EnOpt is more efficient than an adjoint method in terms of simulator requirements. Unlike the adjoint method, EnOpt does not require any access to the simulator source code, thus, treats the simulator as a black box. The main idea of EnOpt is that the gradient is approximated using a linear regression between an ensemble of control parameters and their corresponding objective function values. Thus, the gradient approximation using EnOpt does not depend on the size of control parameters. However, the quality of an approximated gradient depends on the number of realizations contain in the ensemble.

3.1 A Closer Look at EnOpt

Recall the vector of control parameters namely $\boldsymbol{x}$, defined in Section 2.2, which has a size of $1\times N_x$. In this thesis, the objective function to be maximized is the net present value (NPV) of the reservoir, given as

$$g(\boldsymbol{x}) = \sum_{i=1}^{N_t} \frac{v_o Q_{oi}(\boldsymbol{x}) - v_w Q_{wi}(\boldsymbol{x})}{(1 + r_\tau)^{t_i/\tau}} \tag{24}$$

where i is the time step index, N_t is the total number of time steps, r_τ is a discount rate in term of time span τ, and t_i is the cumulative time since the start of the production. v_o and v_w are the price of oil and the cost of water disposal, respectively. Q_{oi} and Q_{wi} are the

total oil and water production over time step Δt_i. It should be pointed out that the objective function $g(\boldsymbol{x})$ used in EnOpt is not limited to the form of NPV, as in (24).

In Section 2.4, we introduced the steepest ascent method which is a method for maximizing the objective function $g(\boldsymbol{x})$. The steepest ascent method use search direction as a gradient of the objective function with respect to the control parameters $\left(\boldsymbol{p}^k = \nabla g\left(\boldsymbol{x}^k\right)\right)$. Here, we modify the original steepest ascent method to be used with EnOpt. Recall the original steepest ascent in (19), Chen (2008) made a modification for EnOpt as follow

$$\boldsymbol{x}^{k+1} = \boldsymbol{x}^k + \alpha^k \left(\boldsymbol{C}_{xx}^k \nabla g\left(\boldsymbol{x}^k\right)\right) \tag{25}$$

We use $\boldsymbol{p}^k = \boldsymbol{C}_{xx}^k \nabla g\left(\boldsymbol{x}^k\right)$ as a search direction instead of $\nabla g\left(\boldsymbol{x}^k\right)$ in original steepest ascent method. The use of ensemble (sample) covariance $\boldsymbol{C}_{xx}$ in front of gradient provides a pre-conditioning for the steepest ascent method. The ensemble (sample) covariance $\boldsymbol{C}_{xx}$ is defined as follow

$$\boldsymbol{C}_{xx} = \frac{1}{N_e - 1}\left(\boldsymbol{X}\boldsymbol{X}^T\right) \tag{26}$$

where $\boldsymbol{X}$ is a mean-shifted ensemble matrix

$$\begin{aligned} \boldsymbol{X} &= \begin{bmatrix} x_{1,1} - \bar{x}_1 & \cdots & x_{N_x,1} - \bar{x}_{N_x} \\ \vdots & \ddots & \vdots \\ x_{1,N_e} - \bar{x}_1 & \cdots & x_{N_x,N_e} - \bar{x}_{N_x} \end{bmatrix} \\ &= \left[\boldsymbol{x}_1 - \bar{\boldsymbol{x}}, \boldsymbol{x}_2 - \bar{\boldsymbol{x}}, \ldots, \boldsymbol{x}_{N_e} - \bar{\boldsymbol{x}}\right]^T \end{aligned} \tag{27}$$

and

$$\bar{\boldsymbol{x}} = \left[\bar{x}_1, \bar{x}_2, \dots, \bar{x}_{N_x}\right] \tag{28}$$

$$\bar{x}_i = \frac{1}{N_e}\sum_{l=1}^{N_e} x_{i,l} \qquad i = 1,2,\dots,N_x \tag{29}$$

The gradient $\nabla g(\boldsymbol{x})$ can be obtained as a least-squares solution (Fonseca et al. 2014) as

$$\nabla g(\boldsymbol{x}) = \left(\boldsymbol{X}^T\boldsymbol{X}\right)^{-1}\boldsymbol{X}^T\boldsymbol{G} \tag{30}$$

where $\boldsymbol{G}$ is a mean-shifted objective function vector, which is defined as follows

$$\boldsymbol{G} = \left[g(\boldsymbol{x}_1) - \bar{g} \quad g(\boldsymbol{x}_2) - \bar{g} \quad \cdots \quad g(\boldsymbol{x}_{N_e}) - \bar{g}\right]^T \tag{31}$$

$$\bar{g} = \frac{1}{N_e}\sum_{l=1}^{N_e} g(\boldsymbol{x}_l) \tag{32}$$

Therefore, (30) can also be expressed as follow

$$\nabla g(\boldsymbol{x}) = \boldsymbol{C}_{xx}^{-1}\boldsymbol{C}_{xg} \tag{33}$$

The cross-covariance matrix $\boldsymbol{C}_{xg}$ is defined in similar a way as the ensemble covariance $\boldsymbol{C}_{xx}$ is defined as,

$$\boldsymbol{C}_{xg} = \frac{1}{N_e - 1}\left(\boldsymbol{X}^T\boldsymbol{G}\right) \tag{34}$$

Hence, the modified steepest ascent in (25) becomes

$$\boldsymbol{x}^{k+1} = \boldsymbol{x}^k + \alpha^k\boldsymbol{C}_{xg}^k \tag{35}$$

Chen (2008) proposed the used of the ensemble covariance $\boldsymbol{C}_{xx}$ as a filtering (smoothing) matrix and the search direction $\boldsymbol{p}^k$ becomes

$$\boldsymbol{p}^k = \boldsymbol{C}_{xx}^k\boldsymbol{C}_{xg}^k \tag{36}$$

Thus, the steepest ascent method used in EnOpt becomes

$$\boldsymbol{x}^{k+1} = \boldsymbol{x}^{k} + \alpha^{k} C_{xx}^{k} C_{xg}^{k} \tag{37}$$

We will use (37) for production optimization throughout this thesis.

3.2 Quality of an Approximated Gradient

Many studies (Fonseca et al. 2015, Fonseca et al. 2013, Stordal et al. 2016) have been done to investigate the effect of the control ensemble to the quality of an approximated gradient. These studies show that the factors that affect the quality of an approximated gradient are sampling techniques, the perturbation size or the variance of the sample distributions, and the size of the ensemble. Fonseca et al. (2015) study the quality of an approximated gradient computed by ensemble method compare to an adjoint method. The author concludes that with proper perturbation size and the number of realizations in the ensemble, the ensemble method gives a good approximation of gradient with an ensemble size that smaller than the size of the control vector.

3.3 Implementation of EnOpt

The procedure of the EnOpt (Chen 2008) is summarized in Figure 3. The optimization uses steepest ascent method to update the control vector $\boldsymbol{x}^{k}$. In each iteration, the search direction $\boldsymbol{p}^{k}$ and the step size α^{k} is determined using (36) and backtracking algorithm with sufficient increase condition, respectively (see Figure 2). Note that we use k as an iteration index: $\boldsymbol{x}^{k}$ is a vector of control parameters at kth iteration, and $\boldsymbol{x}_{l}^{k}$ for $l = 1, 2, \ldots, N_e$ are realizations of the ensemble of control vectors.

1) Let $k = 1$. Generate initial control parameters $\boldsymbol{x}^1$ and initial ensemble of control parameters $\boldsymbol{x}_l^1$ for $l = 1, 2, \ldots, N_e$. Here, the ensemble of control parameters $\boldsymbol{x}_l^1$ is generated in 2 steps. First, a mean control is sampled from a uniform distribution with suitable upper and lower limits. Second, a sample from temporally correlated Gaussian random field with zero mean is added to the mean control.
2) Define initial guess for step size $\bar{\alpha}$ and ρ to update the step size in line search algorithm

Start of Loop: EnOpt

3) If $k \geq 2$, a sample from temporally correlated Gaussian random field with zero mean is added to the control $\boldsymbol{x}^k$ to generate the ensemble $\boldsymbol{x}_l^k$
4) Run the simulator and compute the NPV for each realization of control parameters $g(\boldsymbol{x}_l^k)$ using (24).
5) Compute ensemble covariance $\boldsymbol{C}_{xx}^k$ and the cross-covariance $\boldsymbol{C}_{xg}^k$ using (34)
6) For $k = 1$, the initial step size $\alpha_0^1 = \bar{\alpha}$.
   For $k \geq 2$, compute initial step size α_0^k using (23)

Start of Loop: Backtracking line search algorithm

7) Compute the update control parameter $\boldsymbol{x}^{k+1}$ using (37).
8) Run the simulator and evaluate the objective function $g\left(\boldsymbol{x}^{k+1}\right)$
9) If $g\left(\boldsymbol{x}^{k+1}\right)$ satisfies the sufficient increase condition (22), overwrite $\boldsymbol{x}^k$ with $\boldsymbol{x}^{k+1}$ and let $k = k + 1$. Otherwise keep $\boldsymbol{x}^k$, and replace the step size α with $\rho\alpha$ and go to step 6).

End of Loop: Backtracking line search algorithm

10) Check if stopping criteria are satisfied. If not, go to step 3). Otherwise, set $\boldsymbol{x} = \boldsymbol{x}^k$.

End of Loop: EnOpt

Figure 3: Procedure of ensemble-based optimization (Modified from Chen (2008)).

3.4 Illustrative Examples

In this section, two synthetic examples are considered for demonstrating the performance of EnOpt. The first example is a uniform reservoir with single control step (static control). The second example is a channelized reservoir with multiple control steps. However, since the production optimization problem is usually a high-dimensional nonlinear problem, judging if the optimized objective function has reached its maximum is not easy since the reservoir model and the production optimization itself consist with uncertainties. Instead, the control parameters and objective function value are optimized using EnOpt and compared with a base case.

3.4.1 Uniform reservoir with a single control step

This example is a replicate from Chen (2008) where the optimal solution was known. The example considers a two-dimensional uniform reservoir. The reservoir has the size of $2250\times2250\times30$ ft^3, which is uniformly discretized into 45×45 square grids. The permeability is 100 mD with the porosity of 0.2, and only oil and water are presented in the system. The reservoir has 9 producers and 4 injectors completed in repeated five spot pattern as shown in Figure 4. The injection rate in every injector is fixed at 1125 bbl/day, and the total production rate is equal to total water injection rate. The production rate of all 9 producers are the control parameters for the optimization and fixed over the production time of 1000 days. The optimization objective function for this case is the NPV of the reservoir.

Since the injection and total production rate are both fixed, maximizing the objective function for this case is simply to optimize the time of water breakthrough, which occurs when all producers have same water breakthrough time. Thus, the purpose of this optimization is to allocate the production rate among the 9 producers. The optimization uses EnOpt with 30 control realizations, and the result is compared with an equal rate scenario and the known optimal control from pattern fraction (Chen 2008).

Figure 5 shows the water cuts at producers from equal rate scenario (a), and EnOpt (b). For evenly distributed production rate scenario, producer P1, P3, P7, and P9 have the earliest water breakthrough, followed by producer P2, P4, P6, and P8, and producer P5 has the latest water breakthrough. After optimization has been performed, water breakthrough time in all producers became closer. Figure 6 shows the water saturation at the end of year 1 for both cases. It demonstrates that the EnOpt distributed water more evenly in the reservoir. The production rate from EnOpt, shown in Figure 7, is closed to known optimal solution from pattern fraction (Chen 2008) although not the same. Chen (2008) suggest for this case that changing the objective function to water arrival time might make EnOpt result closer to the optimal solution.

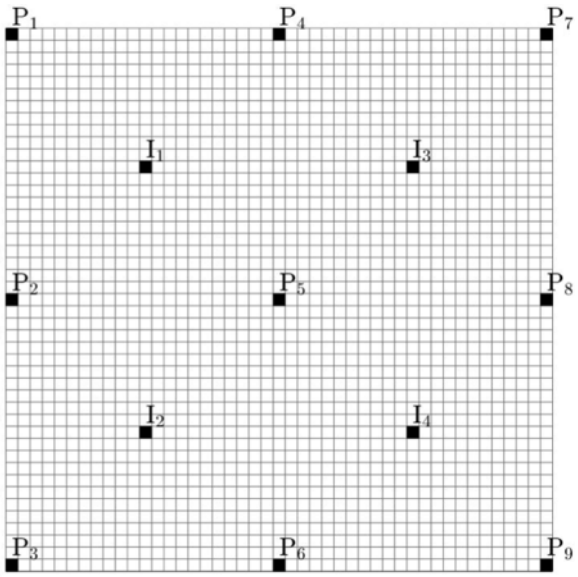

Figure 4: The well locations for uniform permeability case (Modified from Chen (2008)).

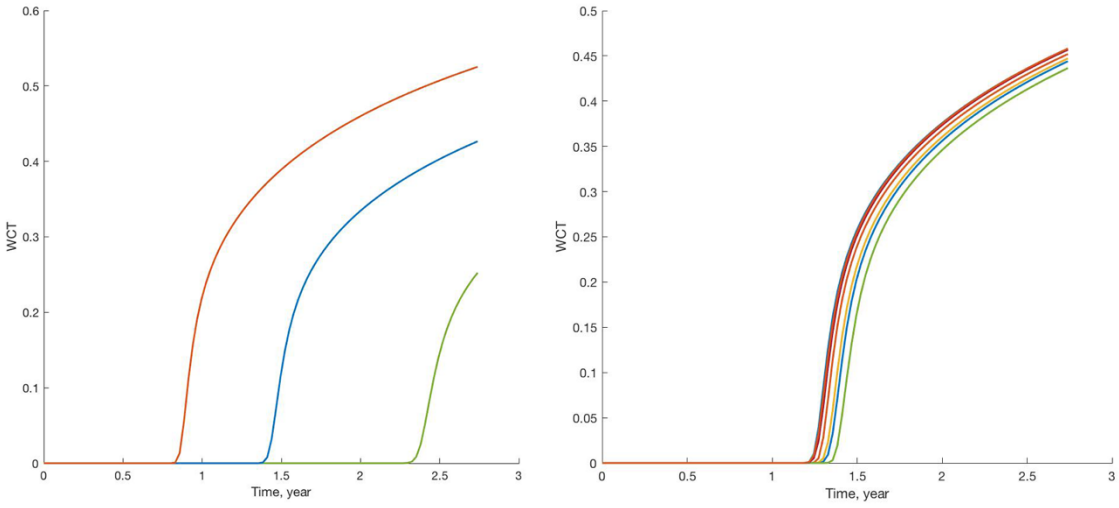

(a) Equals rates control (b) EnOpt

Figure 5: Compare water cuts at 9 producers using different control strategies.

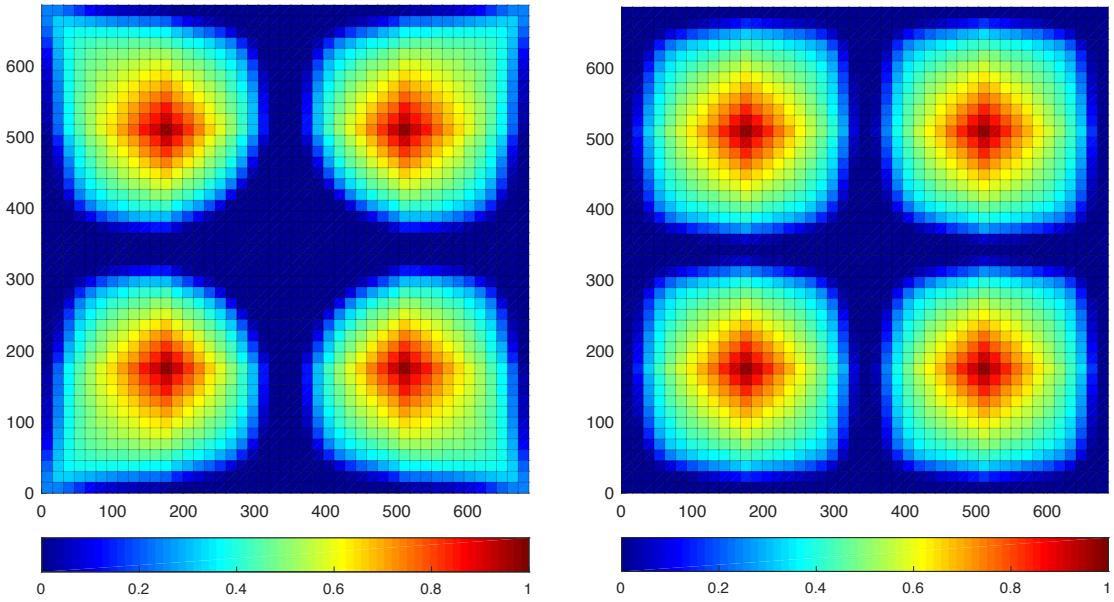

(a) Equals rates control (b) EnOpt

Figure 6: Compare water saturation after 1 year of production using different control strategies

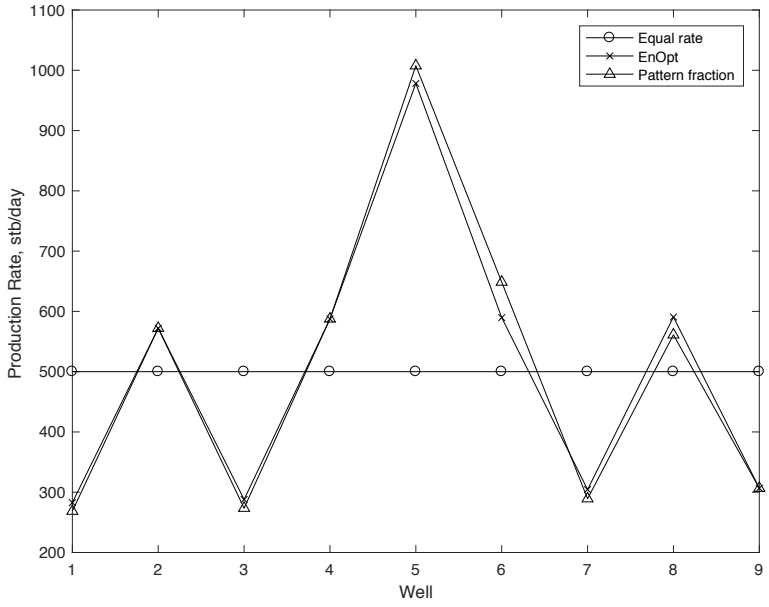

Figure 7: Optimized controls from different control scenarios. EnOpt (diamonds), equal rate scenario (circles), and pattern fraction(triangle).

3.4.2 Channelized reservoir with multiple control steps

In this second example, we consider a 2250×2250×30 ft^3 channelized reservoir, which is uniformly discretized into 45×45 square grids. The reservoir model consists of two facies with uniform properties; a channel sand with a permeability of 8 D and a background shale with a permeability of 10 mD. The permeability field of the reservoir is shown in Figure 8. The porosity is assumed to be uniform and equal to 0.2. The reservoir has 9 producers and 4 injectors completed in repeated five spot pattern. Both injectors and producers are controlled by liquid rates. The total water injection rate is equal to total liquid production rate and equal to 4500 bbl/day. The optimization is done using NPV as an objective function where the oil price is $55/ bbl, and the cost of water disposal is $10/ bbl. The discount rate used in NPV function is 10% per year, and the time frame of the optimization is 1020 days. The control settings are changed every 60 days. Thus, there are 17 control steps, and the total number of control parameters is a product of a number of well and number of control steps, 13×17 = 221.

The initial control is set as an equally distributed injection and production rate scenario. The ensemble of control parameters is generated by adding samples from a temporally correlated Gaussian random field with zero mean to the initial control. For this example, an ensemble of 50 realizations is used. The optimization result is compared with a base case where all total water injection and total liquid production are both equally distributed among the injectors and producers. The goal of this optimization is to redistribute injection and production rate in each well to achieve higher NPV.

Figure 9 shows the changes of NPV with iterations (solid line) compare to the NPV from a based case. The EnOpt is terminated when the increase of NPV is less than 0.01%. The optimization increases the NPV by 4.26% compares to the base case. In Figure 10, it shows that the major contribution of the optimization is to delay and reduce water production while still maintain oil production. The oil recovery is slightly higher (3.36% higher) when the amount of water produced is significantly decreased (10.58% lower). The optimized control settings for injectors and producers are shown in Figure 11 and Figure 12, respectively.

Throughout this section, we have briefly discussed the ensemble-based method for approximation of the gradient to be used in steepest ascent method. Two examples demonstrate that EnOpt successfully optimized the production and higher the NPV. In the next section, we apply the EnOpt into a bigger production scale, a synthesis reservoir, namely UNISIM-I.

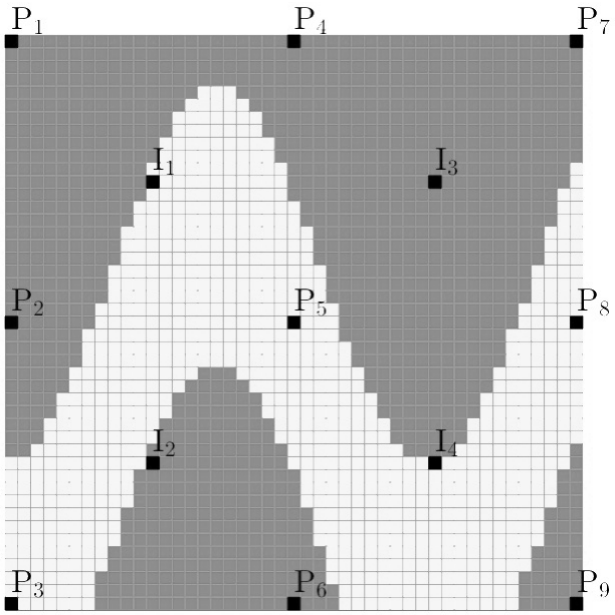

Figure 8: The permeability field of the channelized reservoir with well locations. Gray indicates background shale (10mD) and white indicates channel sand (8 D)

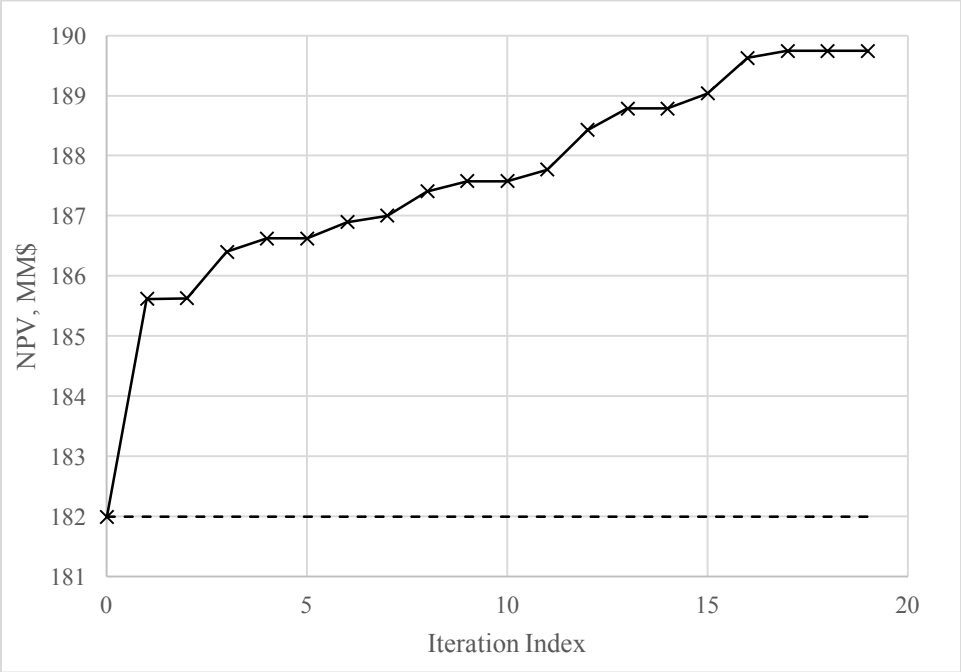

Figure 9: The change of NPV with iterations. The solid line indicates NPV from EnOpt, the dash line indicates NPV from an equal rate case.

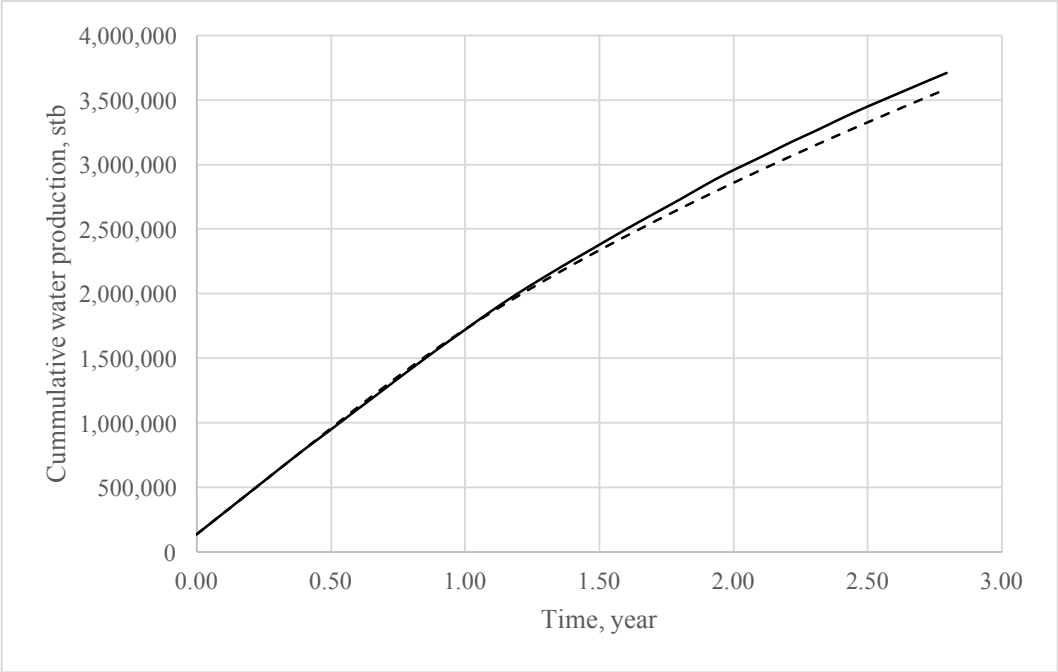

(a) Cumulative oil production

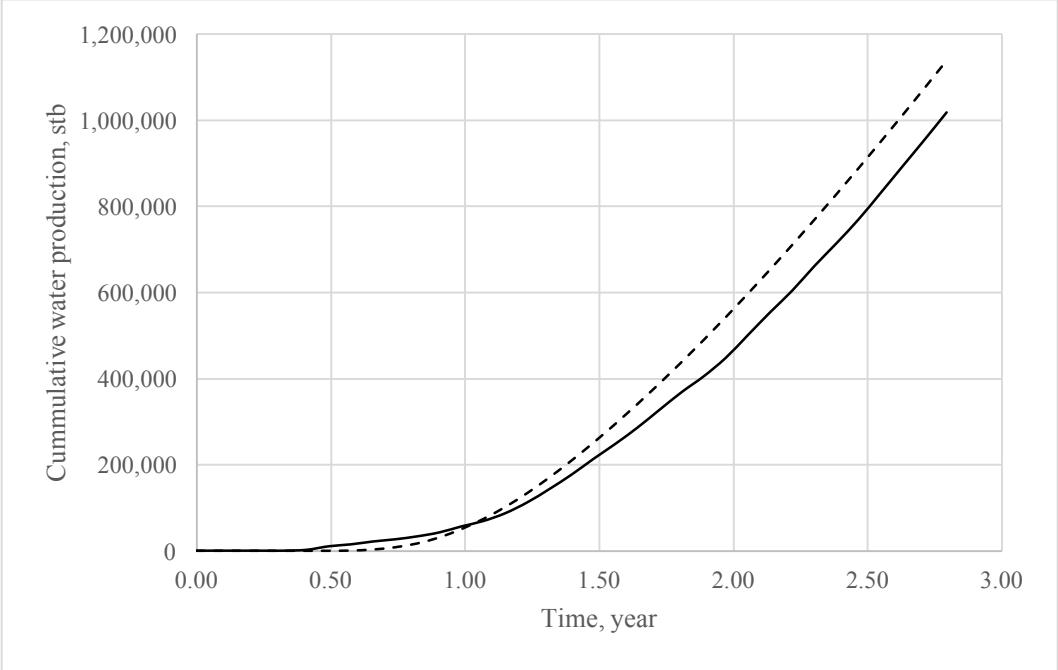

(b) Cumulative water production

Figure 10: Comparison of cumulative oil and water production. The solid line indicates EnOpt result. The dash line indicates base case result.

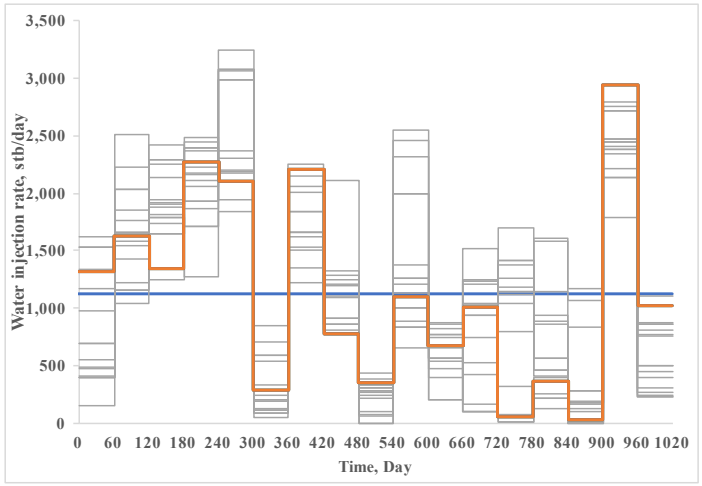

(a) Injector 1

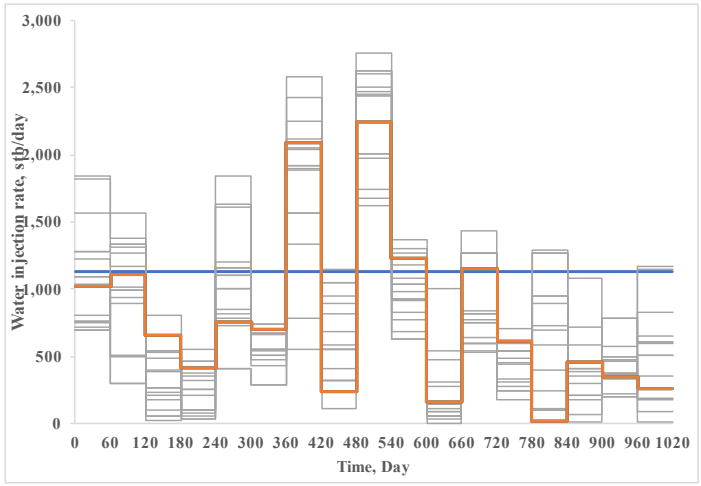

(b) Injector 2

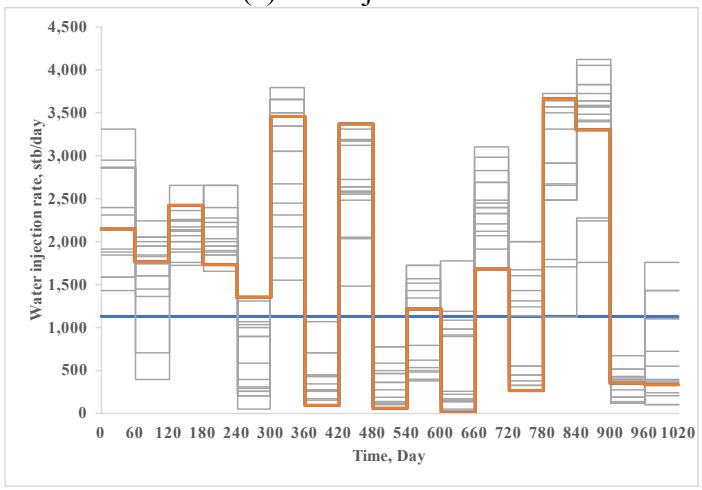

(c) Injector 3

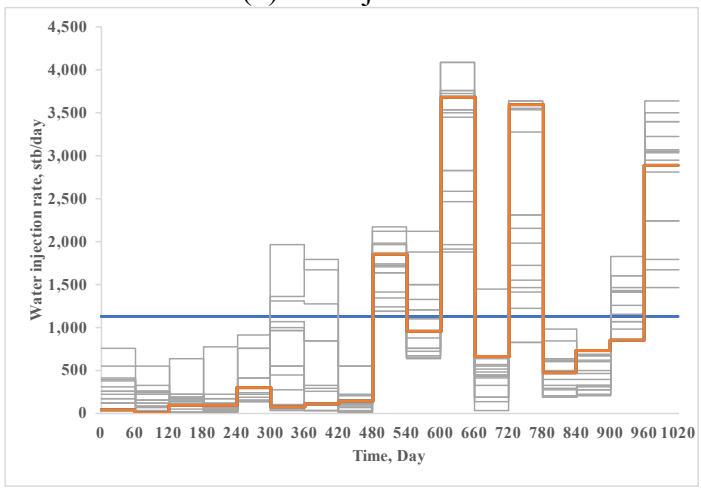

(d) Injector 4

Figure 11: Water injection rate of each injector at each iteration. Blue line indicates a base case, red line indicates optimization result.

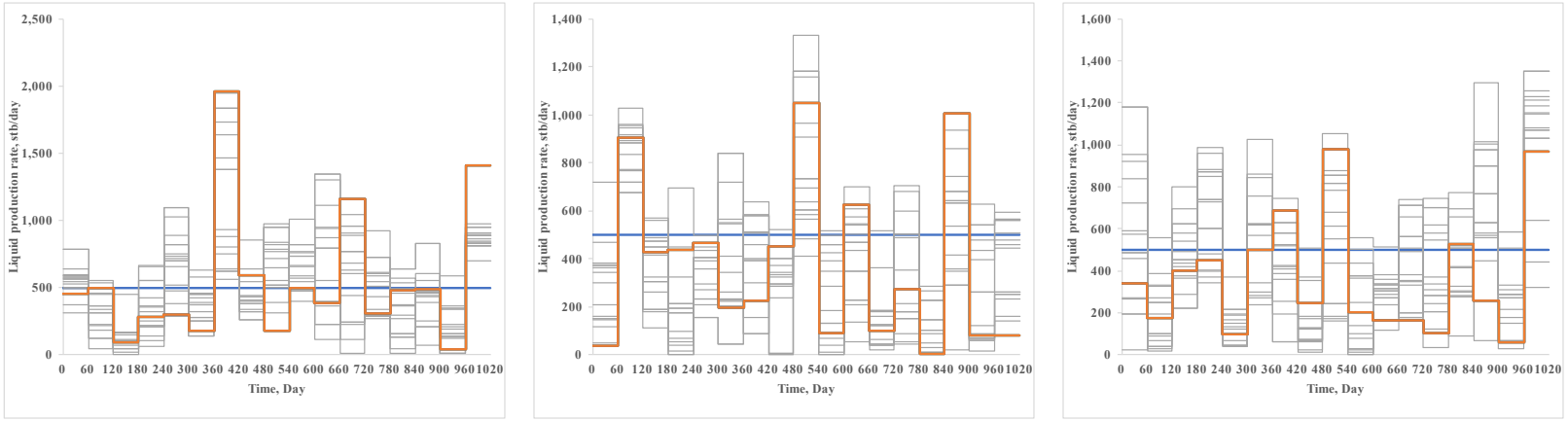

(a) Producer 1 (b) Producer 2 (c) Producer 3

(d) Producer 4 (e) Producer 5 (f) Producer 6

Figure 12: Liquid production rate of each producer at each iteration. Blue line indicates a base case, red line indicates optimization result.

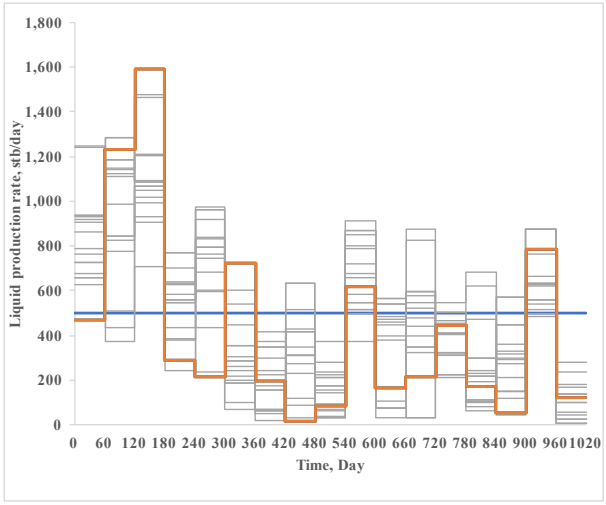

(g) Producer 7

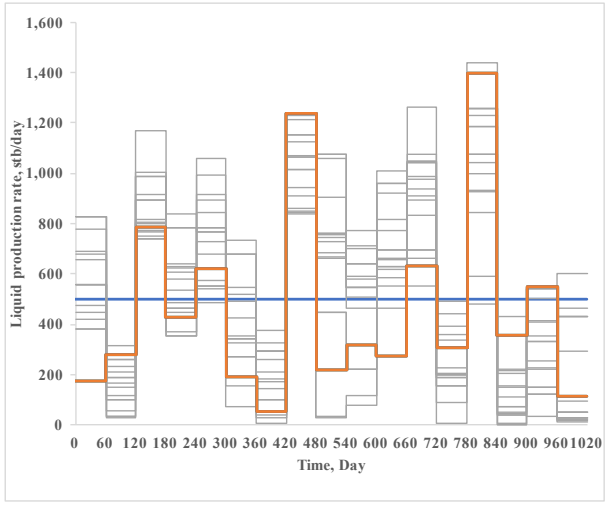

(h) Producer 8

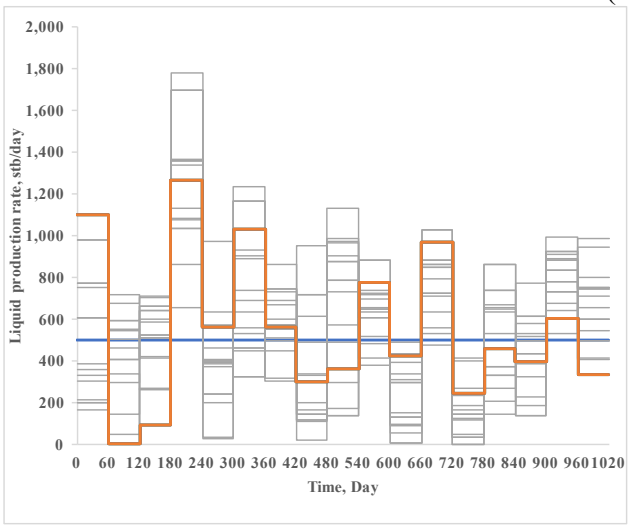

(i) Producer 9

Figure 12: Continued.

4. APPLICATION OF ENSEMBLE-BASED OPTIMIZATION (EnOpt) ON UNISIM-I

4.1 Field Description and Optimization Scheme

In this section, we apply the EnOpt on a larger production scale, UNISIM-I. The UNISIM-I is a synthetic reservoir model designed by UNISIM-Cepetro-Unicamp as a comparative case for reservoir management. The model was built based on the structural, facies and petrophysical model of the Namorado oil field, located in Campos Basin, Brazil with some modifications (Avansi et al. 2015, Gaspar et al. 2016, Gaspar et al. 2015). The original high-resolution model has a dimension of 326×234×157 cells, which approximately 3.4 million of the total cells are active cells. For the optimization case, the model is upscaled into about 37,000 active grid blocks. The field has been developed by 11 injectors and 14 producers. The constraints for injectors and producers are shown in Table 1. Figure 13 and Figure 14 shows the porosity and permeability maps, respectively, with well locations of UNISIM-I reservoir. The fluid system in this problem is incompressible and immiscible and consists of oil and water with some properties shown in Table 2. Figure 15 shows the relative permeability plot of oil and water.

Table 1: Well constraints

Injector	
Water injection rate (m^3/day)	0-5,000
BHP (kgf/cm^2)	Max 350
Producer	
Liquid production rate (m^3/day)	0-2,000
BHP (kgf/cm^2)	Min 190

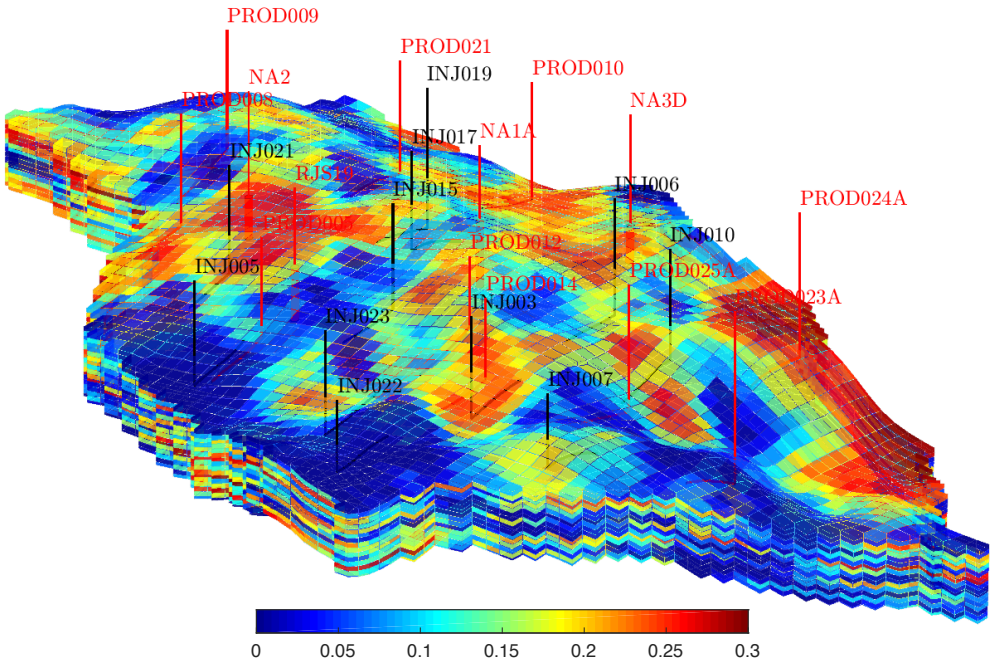

Figure 13: Porosity map with well locations of UNISIM-I reservoir. Producers are indicated in red, and injectors are indicated in black.

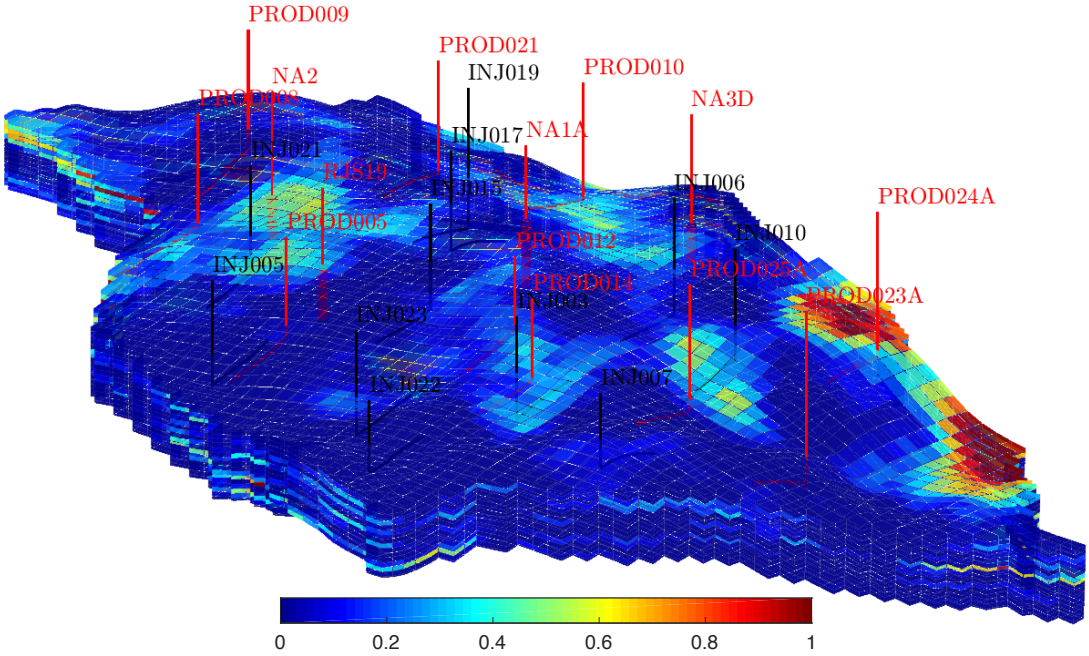

Figure 14: Permeability map with well locations of UNISIM-I reservoir. Producers are indicated in red, and injectors are indicated in black.

Table 2: Fluid properties

	Water	Oil
Viscosity (cP)	1	5
Density (kg/m^3)	1,014	850
Residual water saturation (S_{wr})	0.2	-
Residual oil saturation (S_{or})	-	0.2

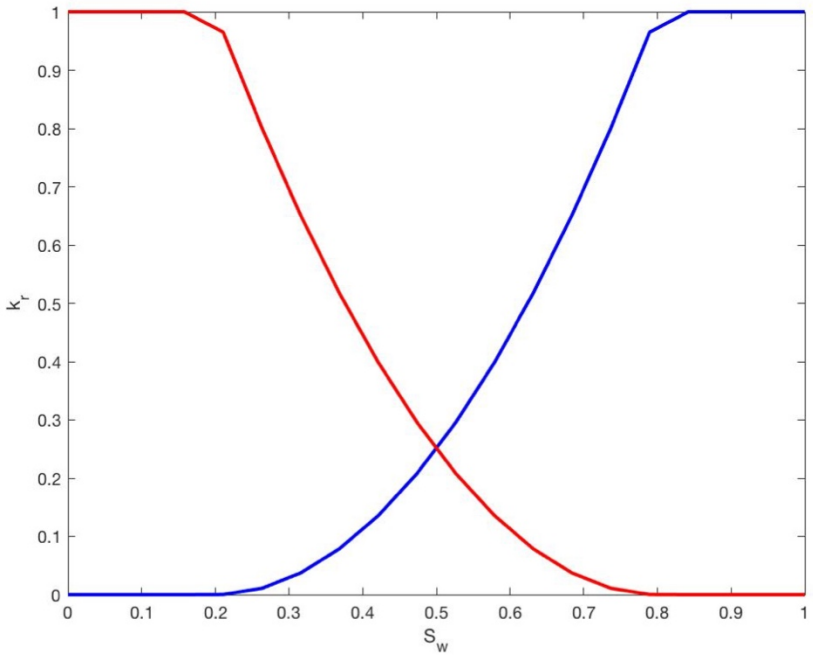

Figure 15: Relative permeability plot of water (blue) and oil (red).

We use EnOpt to optimize the production of UNISIM-I by changing the injection and production schedule of the wells. The rates in all wells are changed every 1 year. Hence, the total control parameters in the control vector $\boldsymbol{x}$ for the optimization problem is $25\times20 = 500$ control parameters. The ensemble of control parameters is generated by adding samples from a temporally correlated Gaussian random field with zero mean to the control vector. We use a 100-realization control ensemble to approximate the gradient.

The objective function to be maximized in the optimization of UNISIM-I production is the net present value (NPV) of the reservoir, recall from Section 3.1,

$$g(\boldsymbol{x}) = \sum_{i=1}^{N_t} \frac{v_o Q_{oi}(\boldsymbol{x}) - v_w Q_{wi}(\boldsymbol{x})}{(1 + r_\tau)^{t_i/\tau}} \tag{38}$$

The oil price v_o and the water disposal cost v_w used for calculating the NPV are \$55 and \$10, respectively. We test the EnOpt on 3 optimization scenarios. The first case is a case where all 500 initial control parameters are generated randomly. In the second case, we use a production data at the end of the production history provided in UNISIM-I-M case (Gaspar et al. 2016) to generate an initial control setting. For the first two cases, the discount rate r_τ is 10% per year. In the last case, we run 2 optimizations with different discount rates. Therefore, the goal of this last case is to study how the optimal result is affected by different discount rate.

4.2 Optimization with Random Initial Control Settings

In the first case, we test EnOpt on UNISIM-I with random initial control settings. The production rate in each producer is randomly sampled from the uniform distribution with the upper and lower limits equal to the rate constraints of each well. This initial control is also used as a base case. Figure 16 and Figure 17 show the initial control settings with some realizations from initial control ensemble of the producers and injectors, respectively.

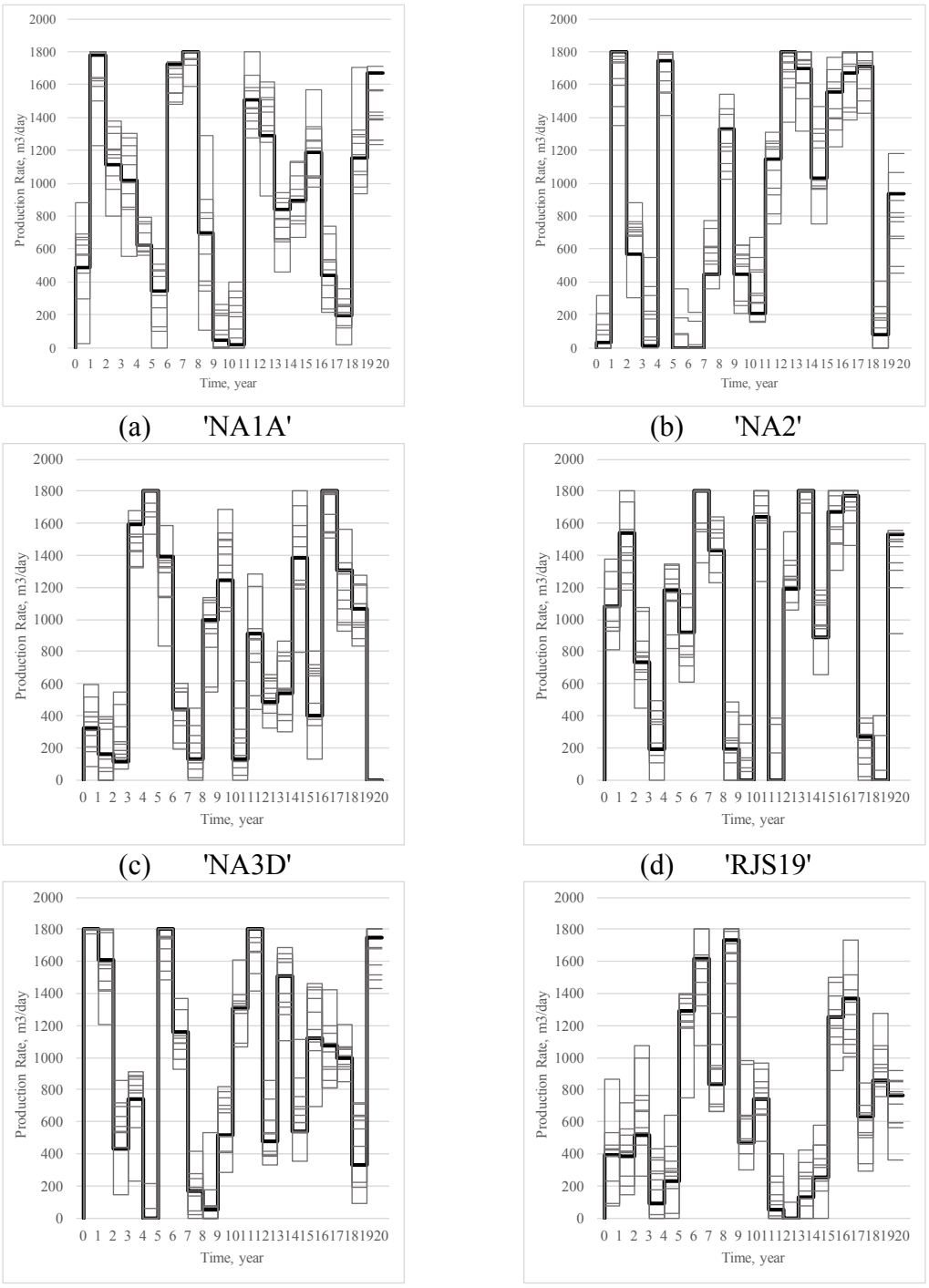

Figure 16: Initial liquid production rates (black) and some realizations from an initial control ensemble (gray) in all producers. The well locations are shown in Figure 13.

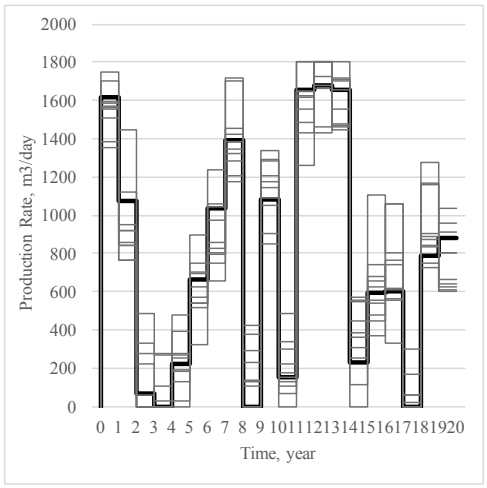

(g) 'PROD009'

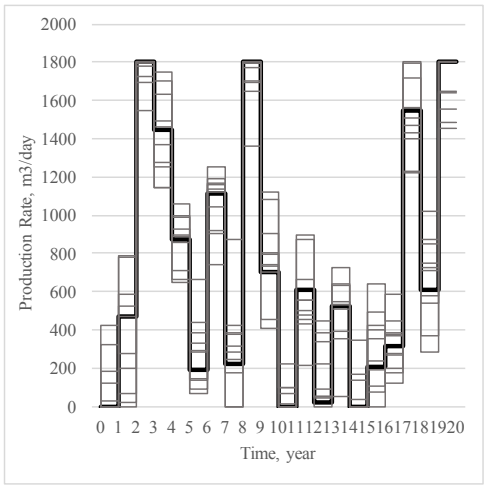

(h) 'PROD010'

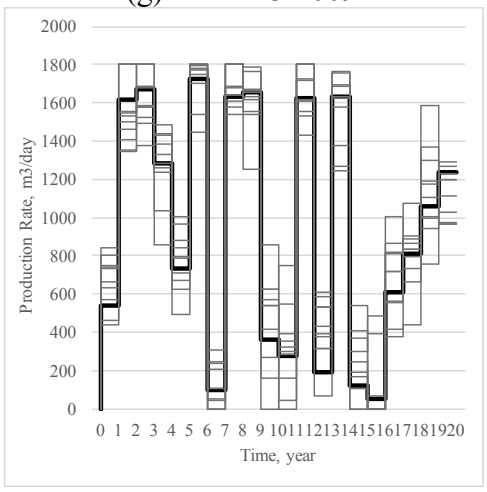

(i) 'PROD012'

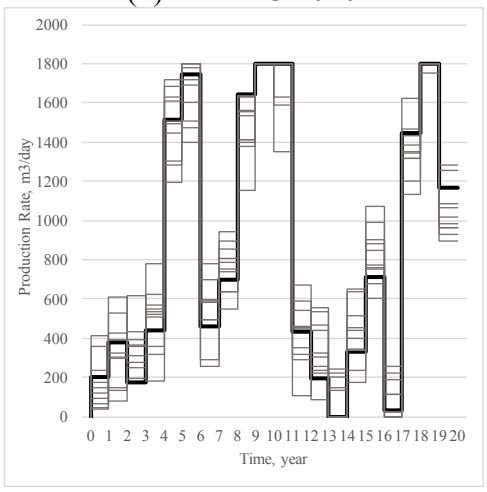

(j) 'PROD014'

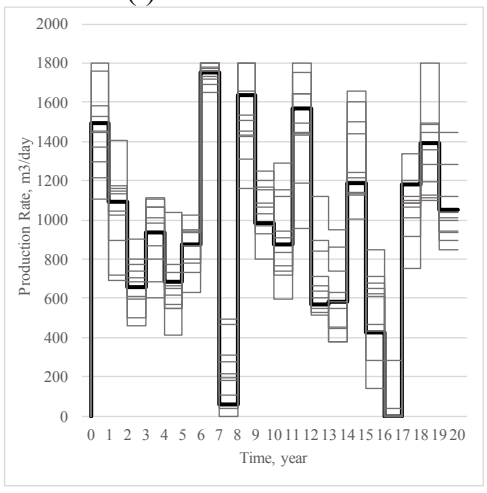

(k) 'PROD021'

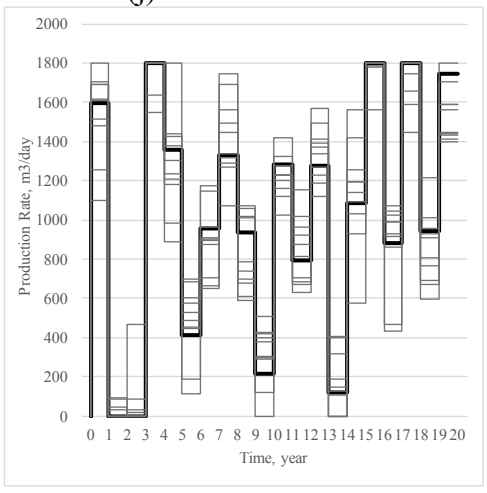

(l) 'PROD023A'

Figure 16: Continued.

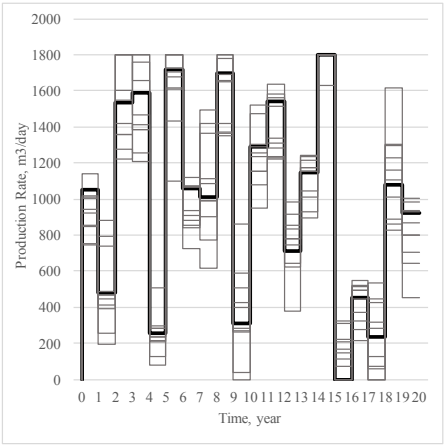

(m) 'PROD024A'

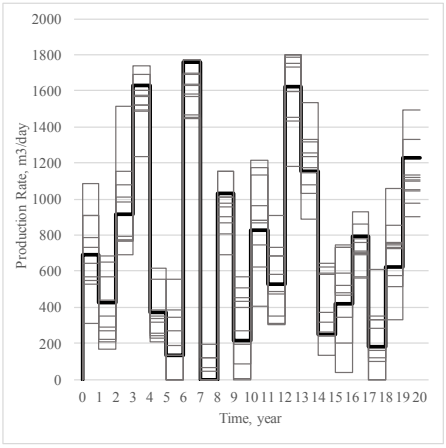

(n) 'PROD025A'

Figure 16: Continued.

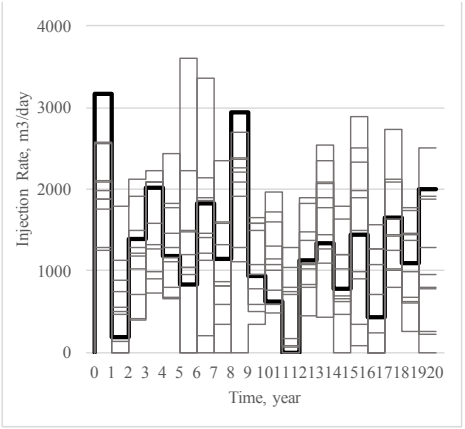

(a) 'INJ003'

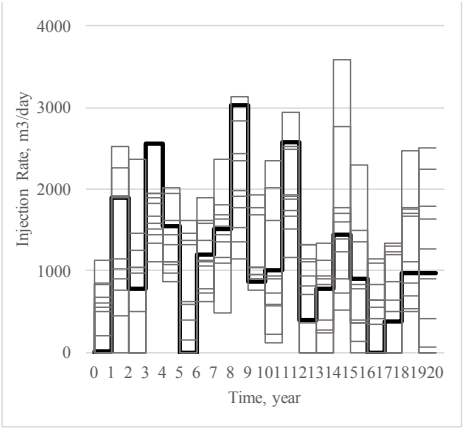

(b) 'INJ005'

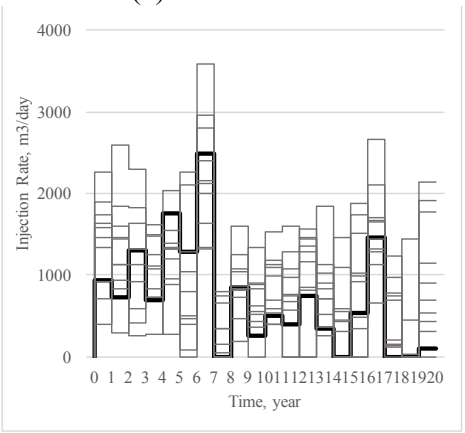

(c) 'INJ006'

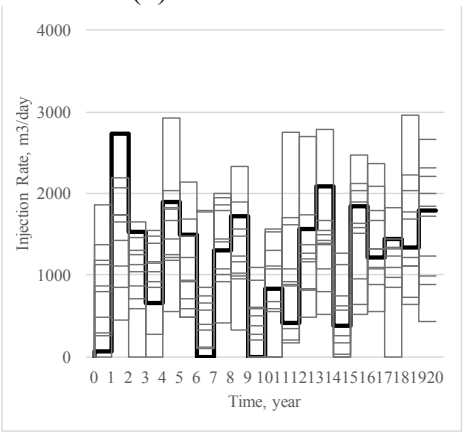

(d) 'INJ007'

Figure 17: Initial water injection rates (black) and some realizations from an initial control ensemble (gray) in all injectors. The well locations are shown in Figure 13.

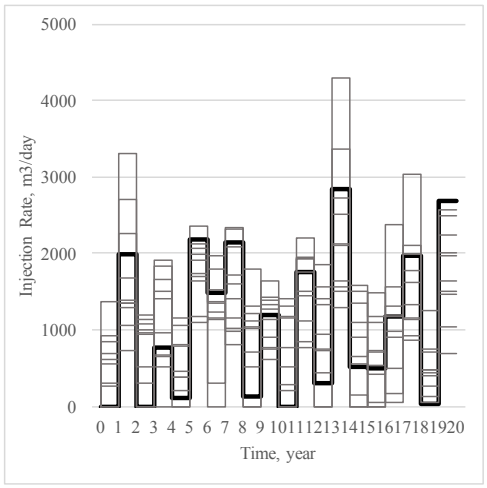

(e) 'INJ010'

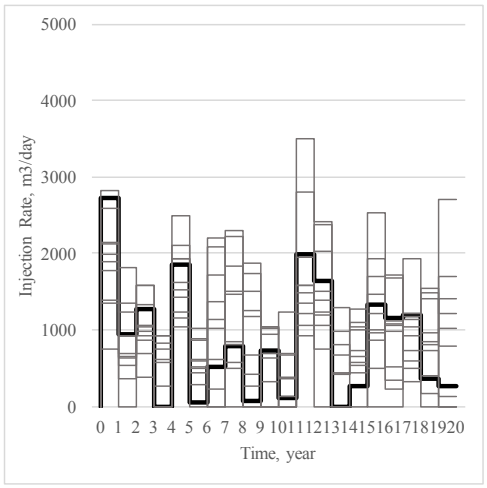

(f) 'INJ015'

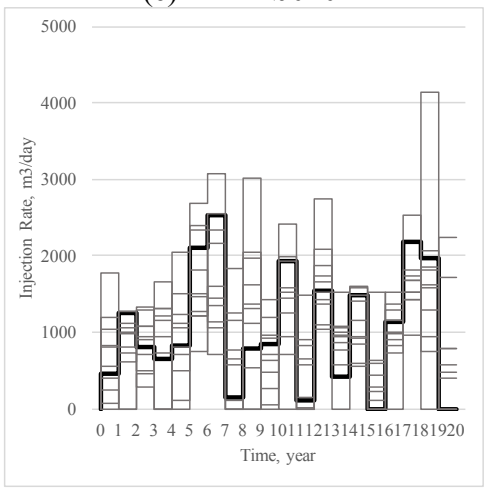

(g) 'INJ017'

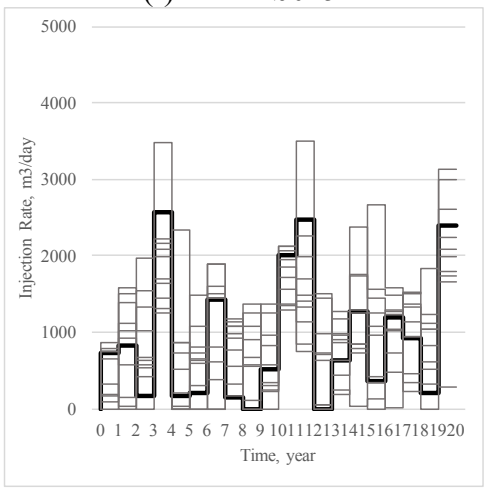

(h) 'INJ019'

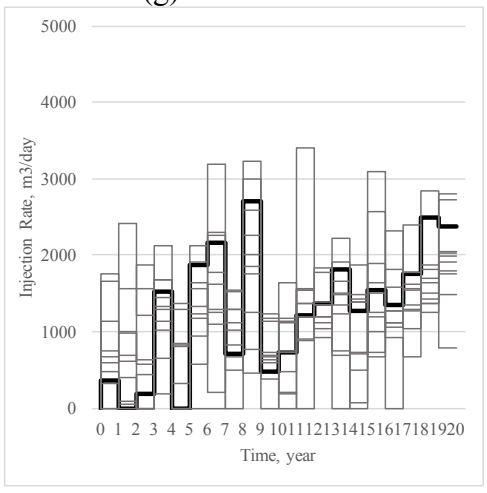

(i) 'INJ021'

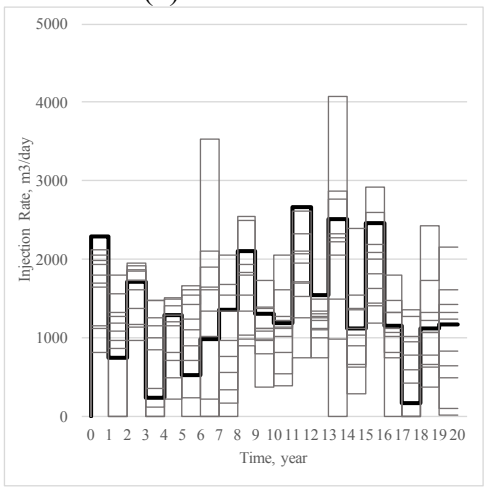

(j) 'INJ022'

Figure 17: Continued.

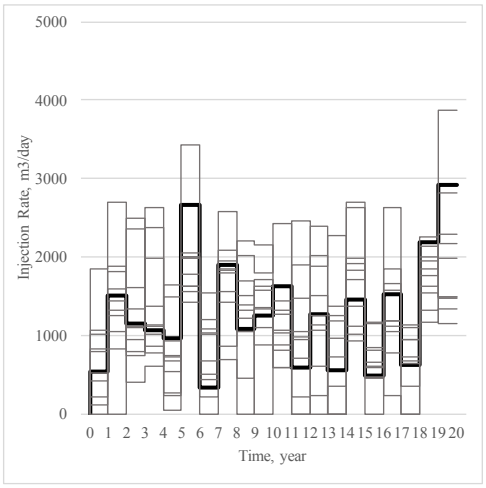

(k) 'INJ023'

Figure 17: Continued.

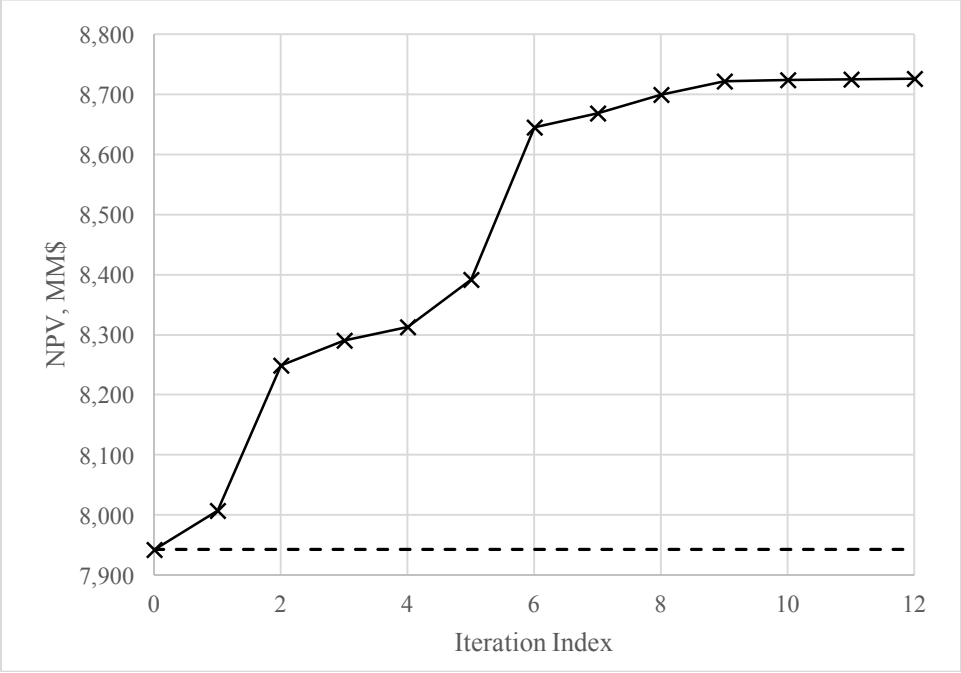

Figure 18: The change of NPV of UNISIM-I reservoir with iterations. The solid line indicates NPV from EnOpt, the dash line indicates NPV from an equal rate case.

The EnOpt increases the NPV of the reservoir from $7.43 billion to $8.73 billion, about 9.87% increase. The optimization converges in 12 iterations. Figure 18 shows the change of NPV with the iterations. The cumulative production for oil and water are shown in Figure 19 and Figure 20, respectively. The total oil production increases from 49.1 MM m^3 to 51.2 MM m^3 while the water production increases from 40.5 MM m^3 to 46.7 MM m^3. Figure 21 compares changes of water saturation in some layer with the production time from a base case and the EnOpt result. These changes in water saturation, from low to high, reflect the oil replacement in the reservoir by the water flooding process. Because the EnOpt increases both oil and water production, we can see that the water saturation maps for EnOpt case indicate higher water saturation in all three layers shown in the figure.

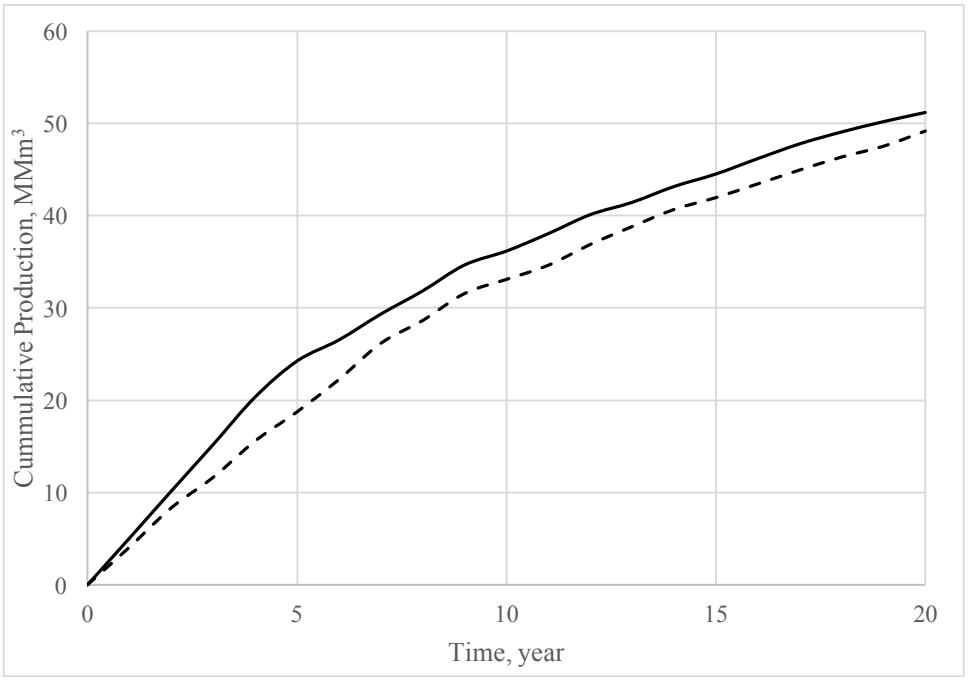

Figure 19: Comparison of cumulative oil production. The solid line indicates EnOpt result. The dash line indicates base case result.

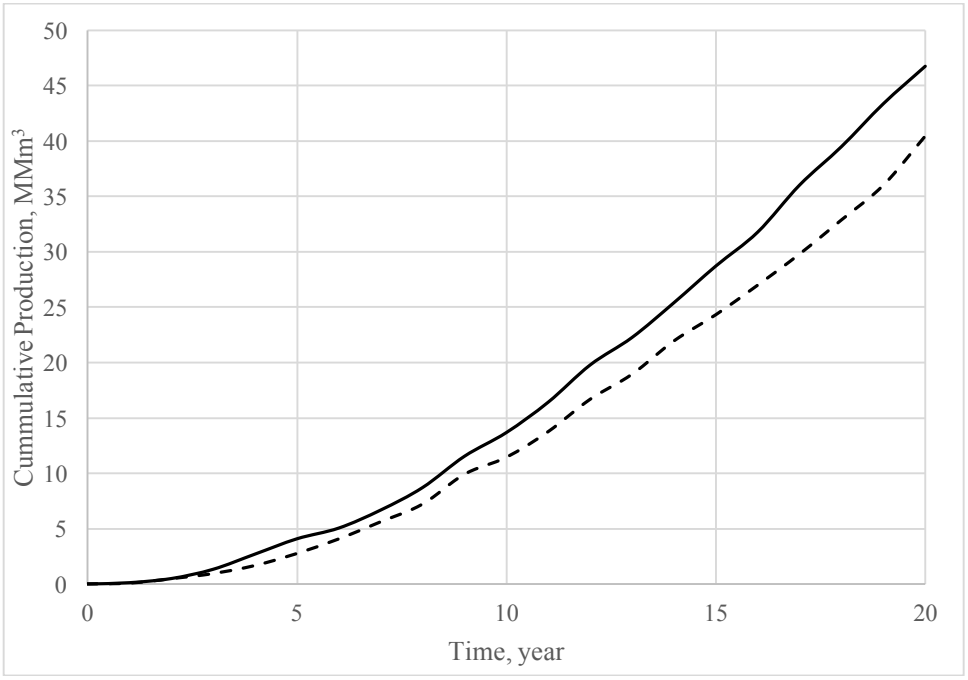

Figure 20: Comparison of cumulative water production. The solid line indicates EnOpt result. The dash line indicates base case result.

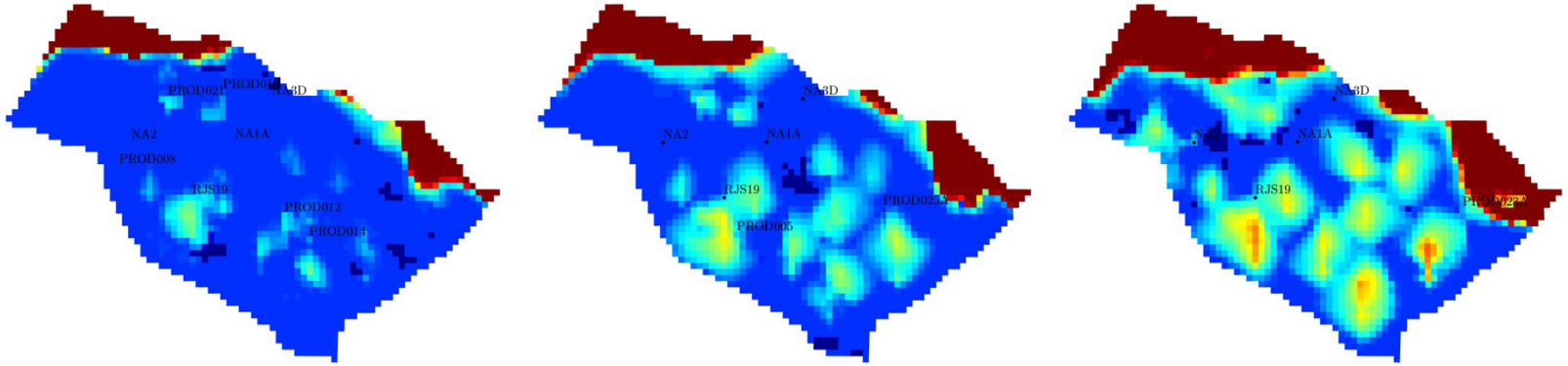

Top layer Layer 3 Layer 8

(a) Base case at 5 year

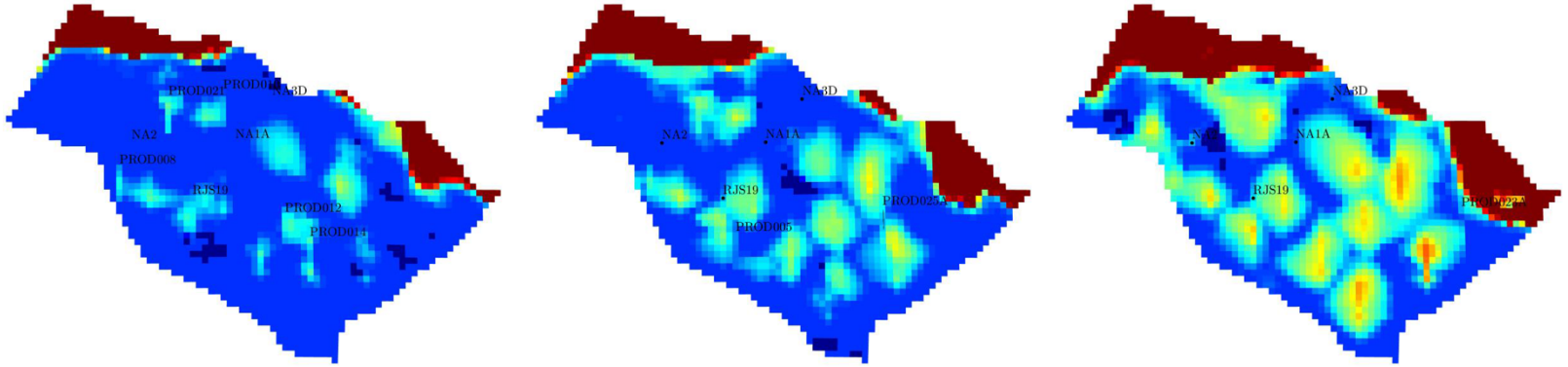

Top layer Layer 3 Layer 8

(b) EnOpt at 5 year

Figure 21: Saturation maps of some layers at different production time.

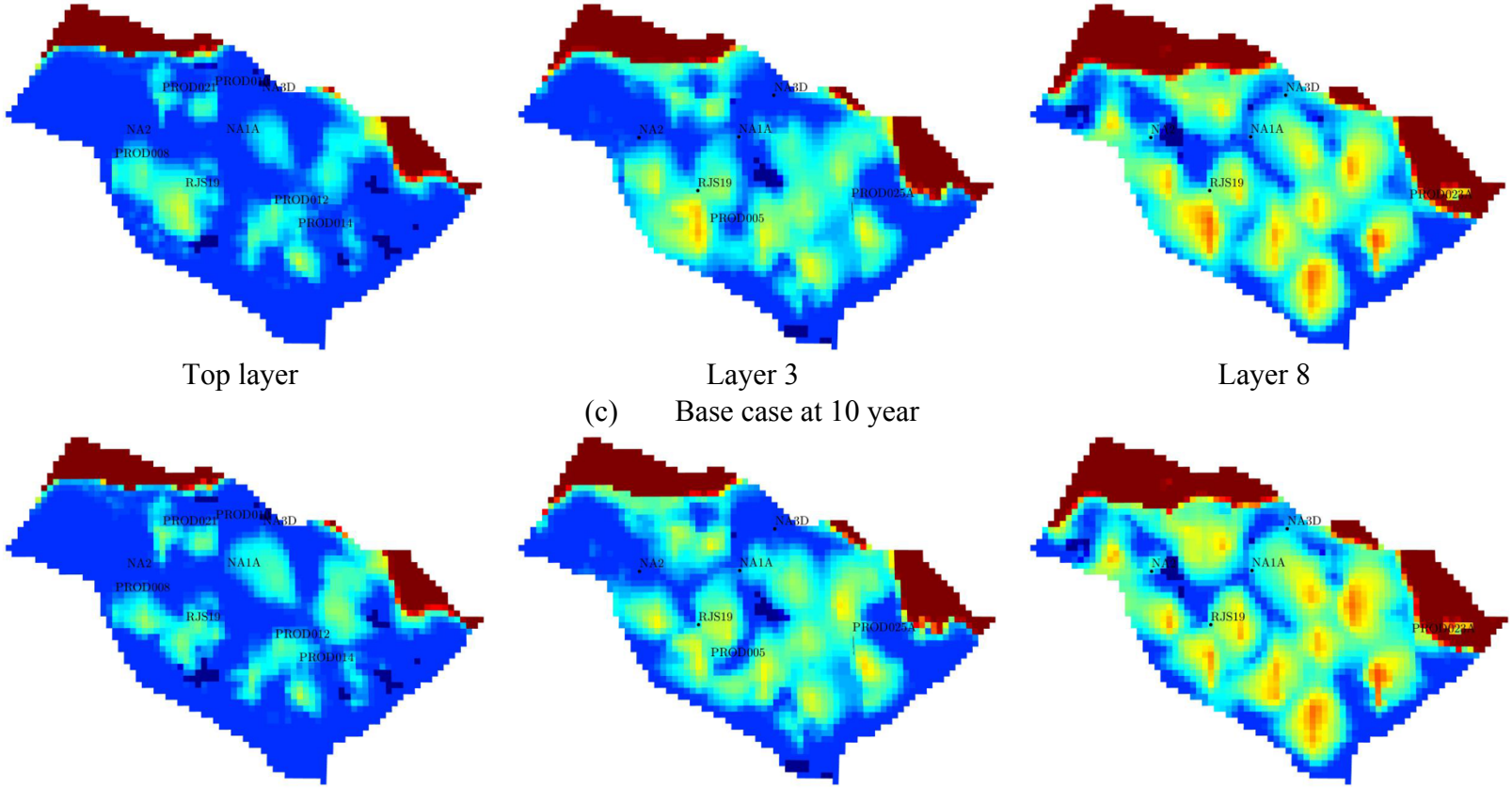

Top layer Layer 3 Layer 8

(c) Base case at 10 year

Top layer Layer 3 Layer 8

(d) EnOpt at 10 year

Figure 21: Continued.

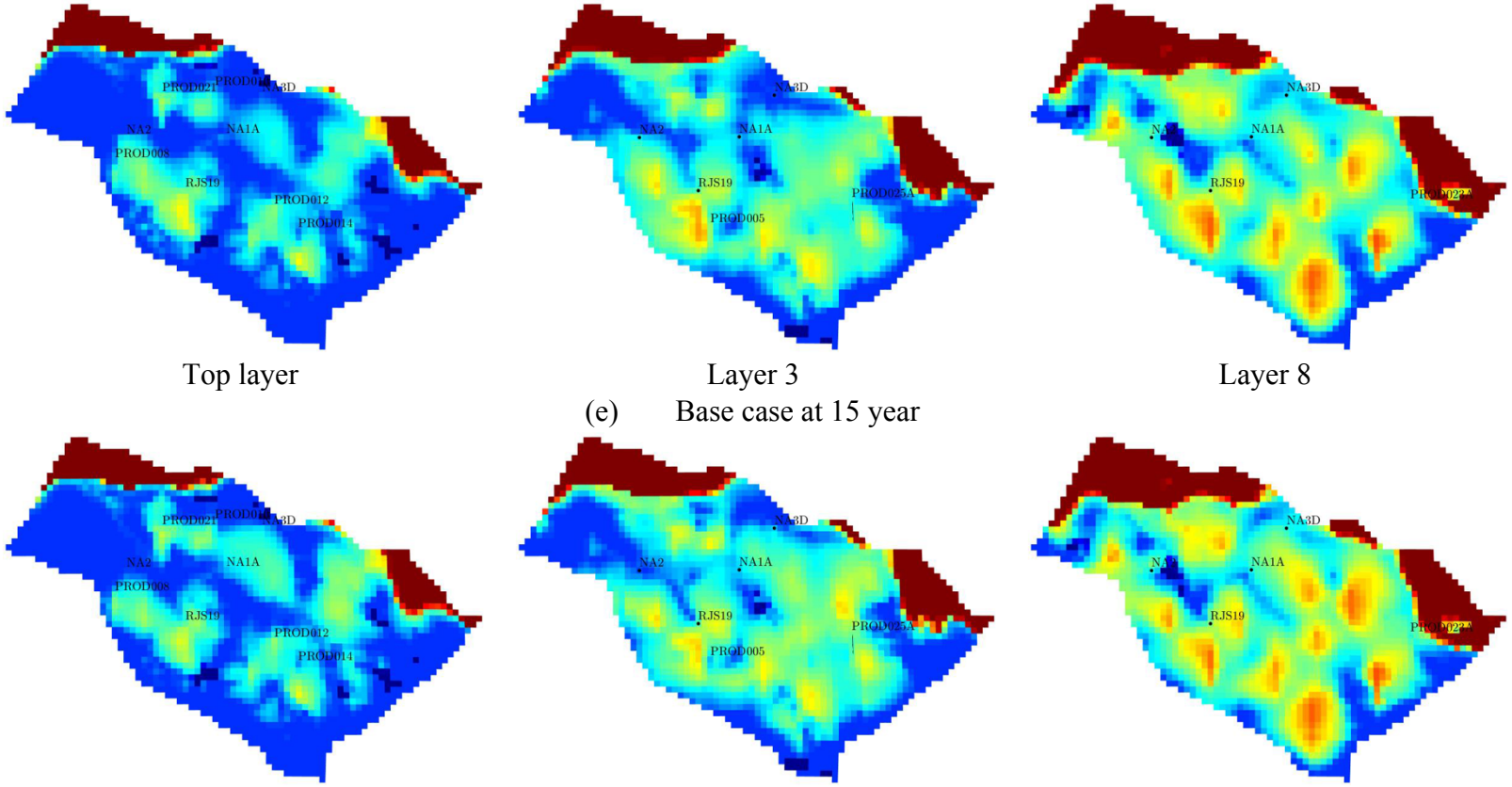

Top layer Layer 3 Layer 8

(e) Base case at 15 year

Top layer Layer 3 Layer 8

(f) EnOpt at 15 year

Figure 21: Continued.

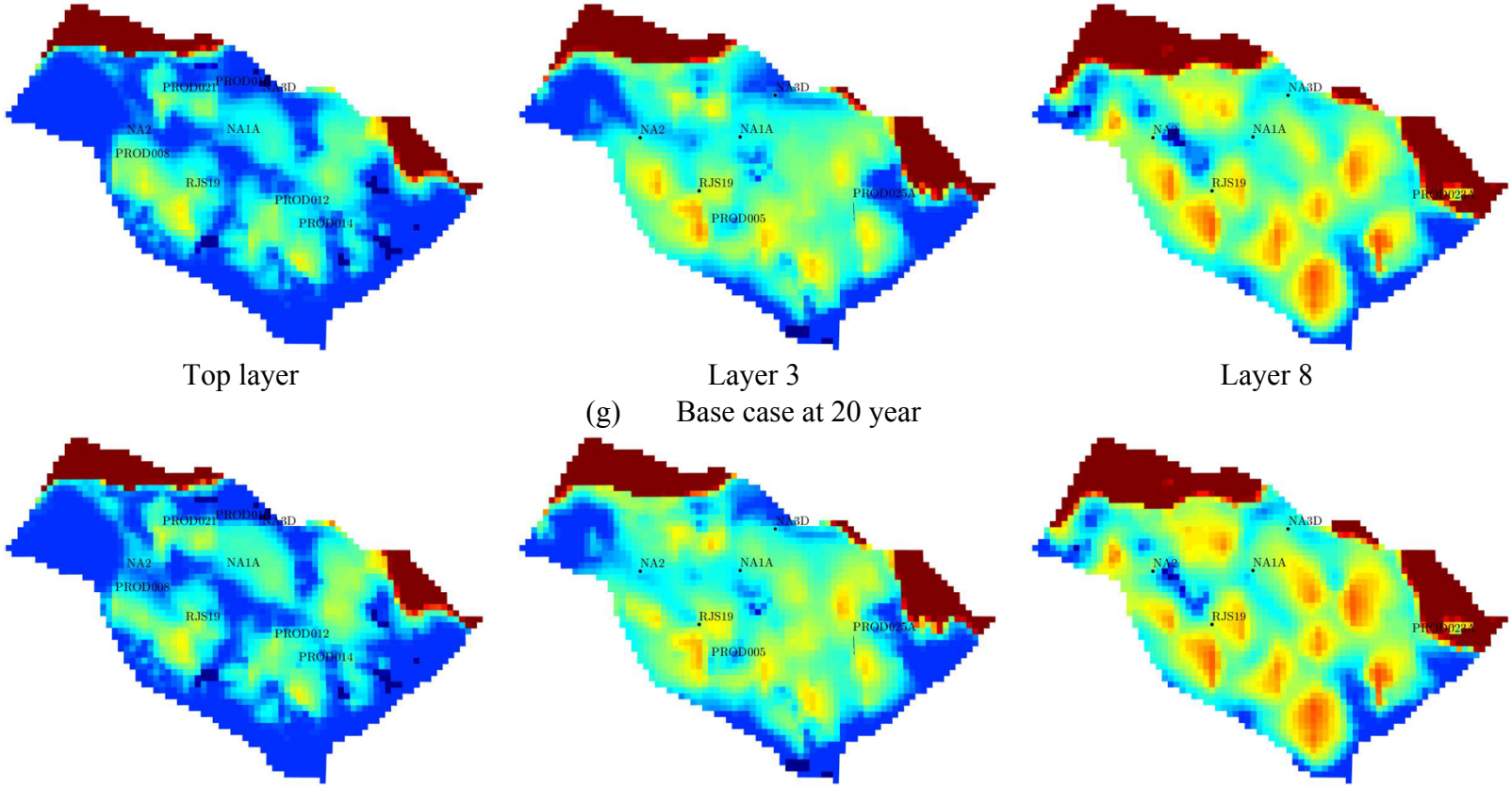

Top layer Layer 3 Layer 8

(g) Base case at 20 year

Top layer Layer 3 Layer 8

(h) EnOpt at 20 year

Figure 21: Continued.

4.3 Extended Production History from UNISIM-I-M

For a more realistic optimization scenario, we use EnOpt to optimize a production of UNISIM-I when the production history is known. In this case, the optimization result is compared with a case where the production schedule is extended from the end of production history. Every well is assumed to have constant injection and production rate from the end of production history throughout the production time of 20 years. Figure 22 and Figure 23 show liquid production and water injection rates of the initial, some iterations, and the optimal controls.

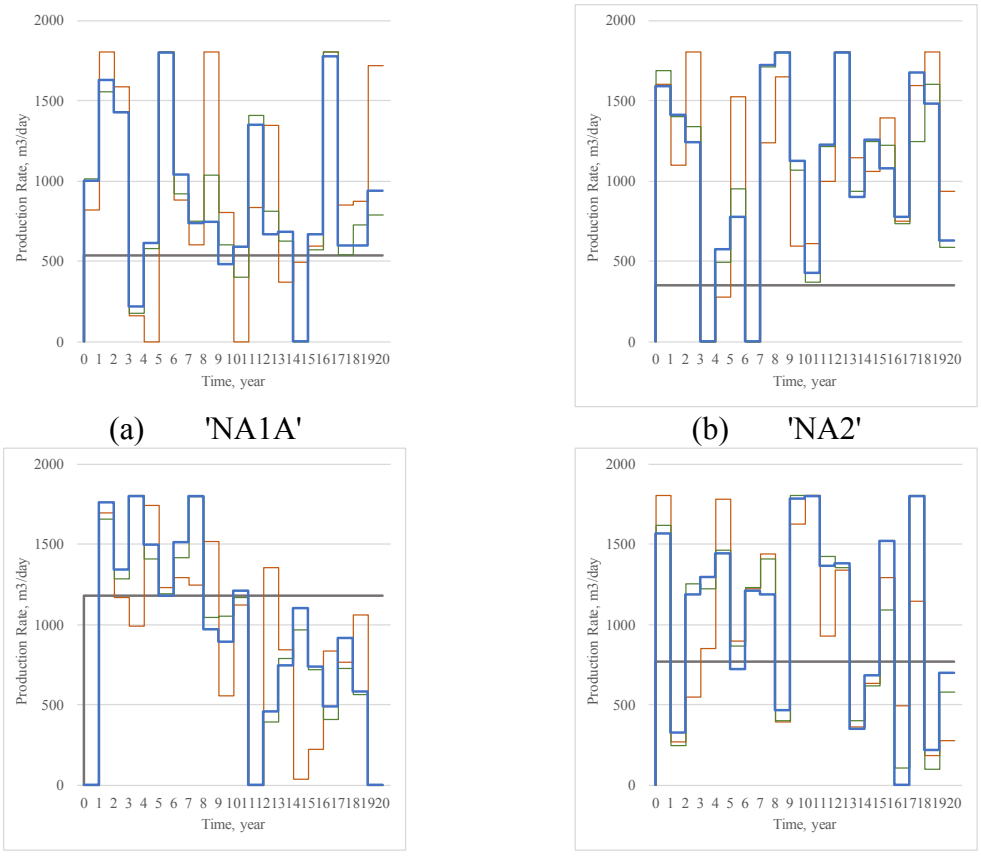

Figure 22: Initial liquid production rates, the 2nd- and 4th-iteration, and EnOpt result. The well locations are shown in Figure 13.

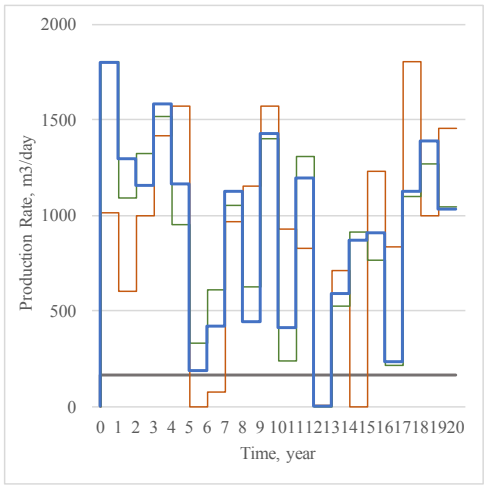

(e) 'PROD005'

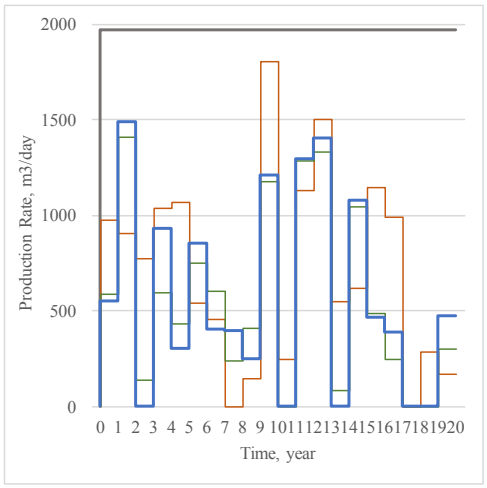

(f) 'PROD008'

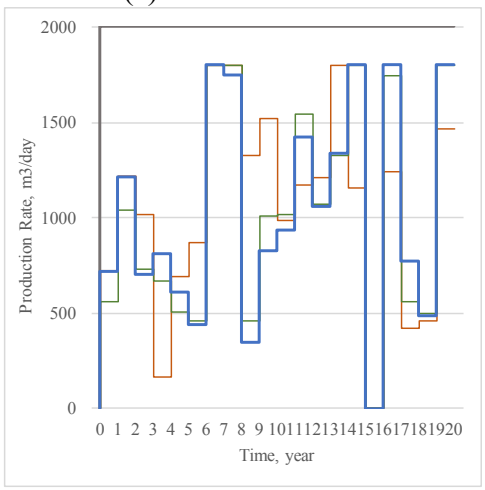

(g) 'PROD009'

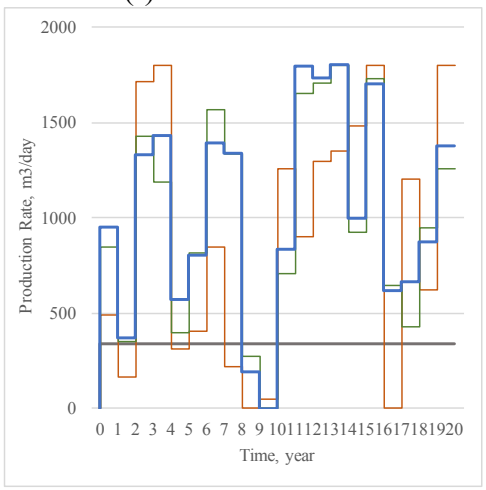

(h) 'PROD010'

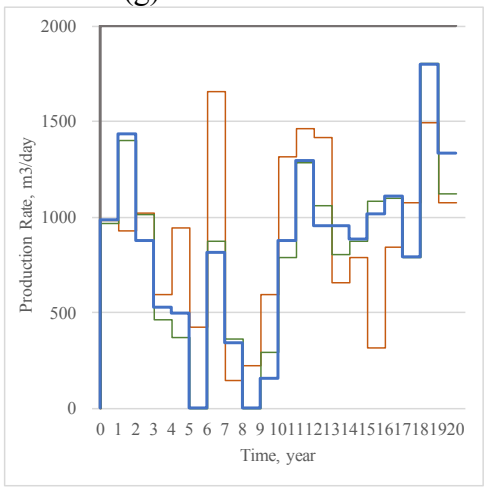

(i) 'PROD012'

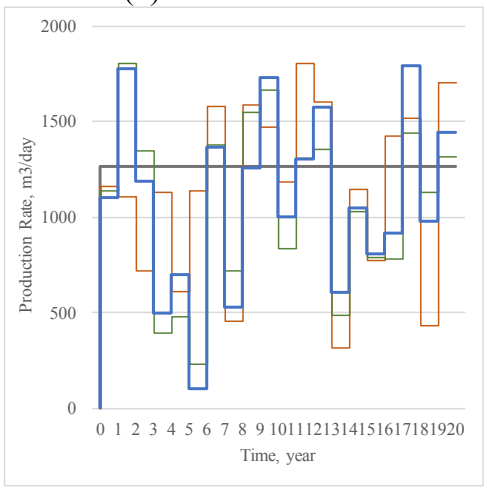

(j) 'PROD014'

Figure 22: Continued.

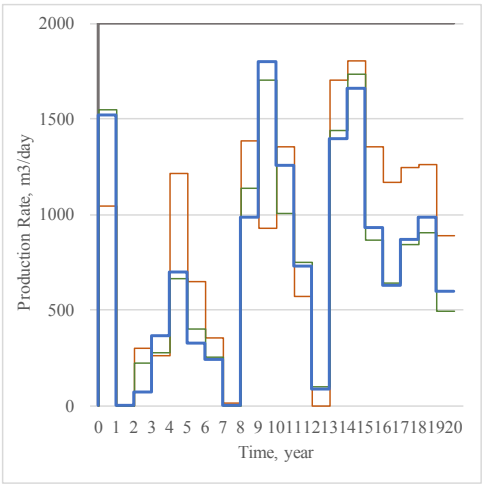

(k) 'PROD021'

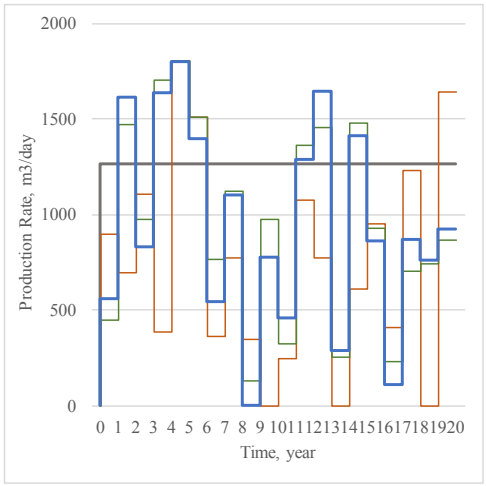

(l) 'PROD023A'

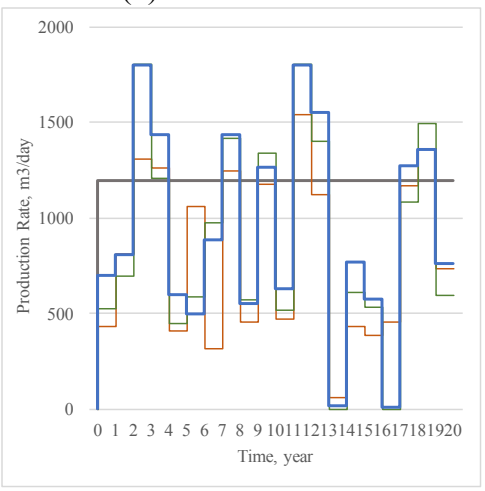

(m) 'PROD024A'

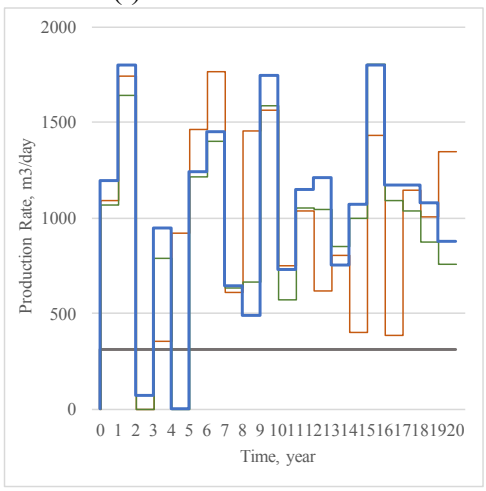

(n) 'PROD025A'

Figure 22: Continued.

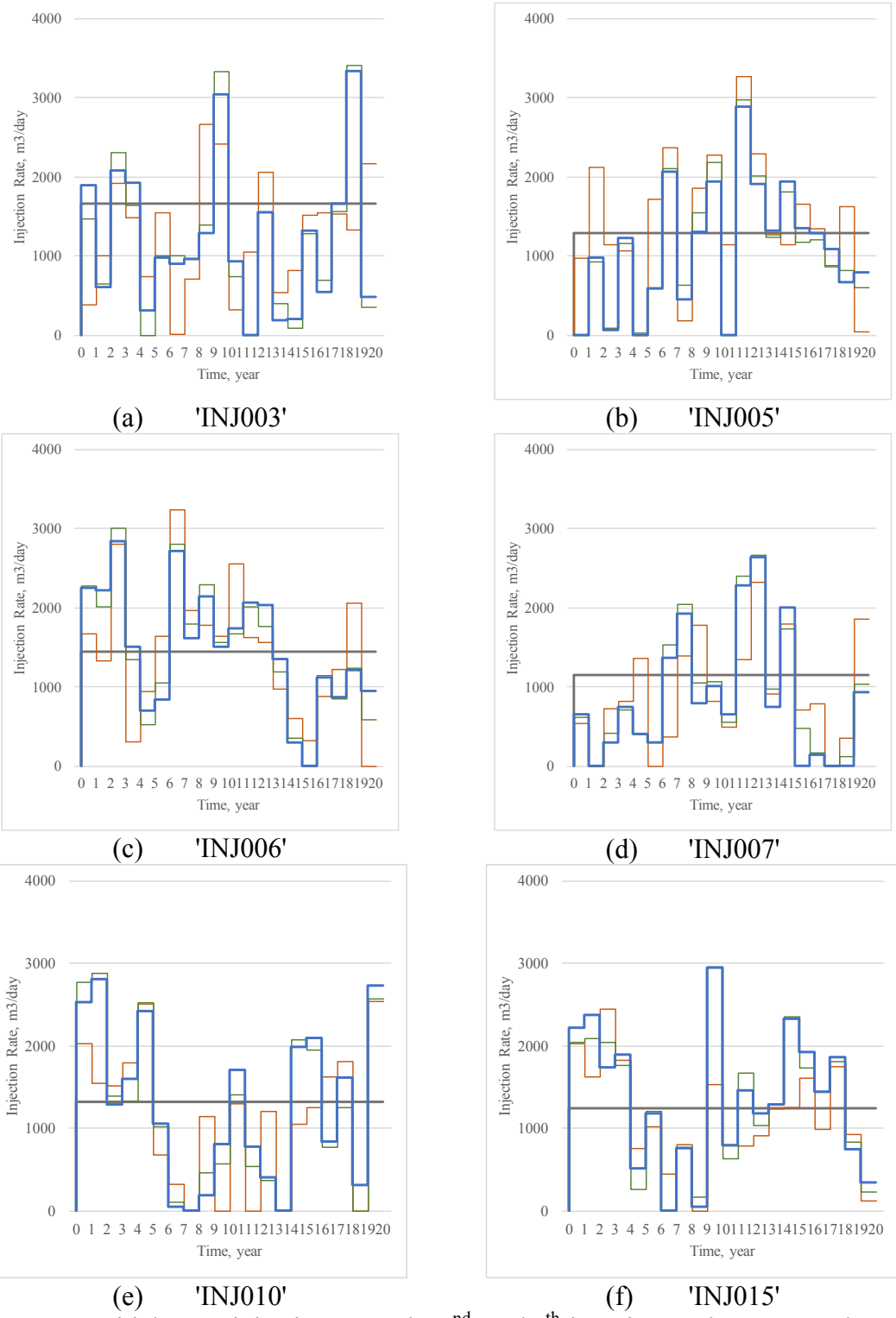

(a) 'INJ003' (b) 'INJ005'

(c) 'INJ006' (d) 'INJ007'

(e) 'INJ010' (f) 'INJ015'

Figure 23: Initial water injection rates, the 2nd- and 4th-iteration, and EnOpt result. Gray line indicates initial injection rate. Orange, green, blue lines indicate 2nd-, 4th-iteration, and EnOpt result, respectively. The well locations are shown in Figure 13.

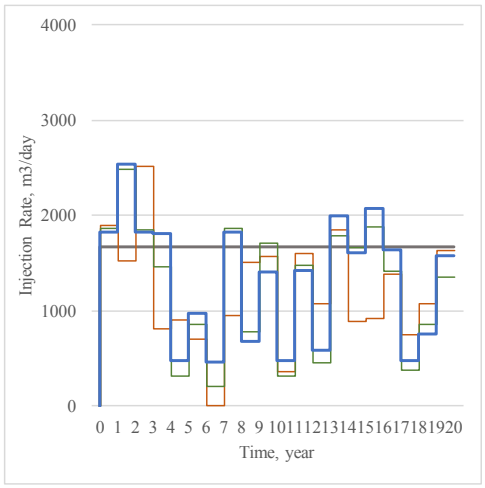

(g) 'INJ017'

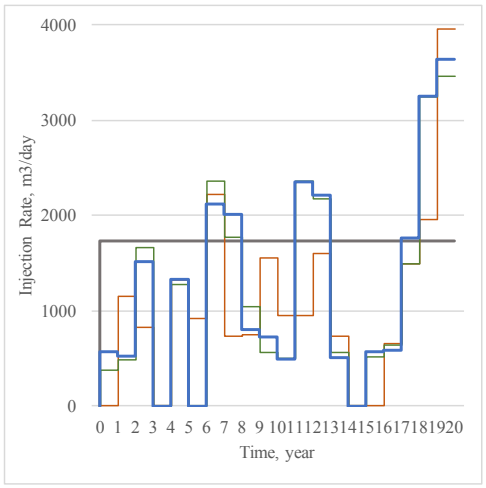

(h) 'INJ019'

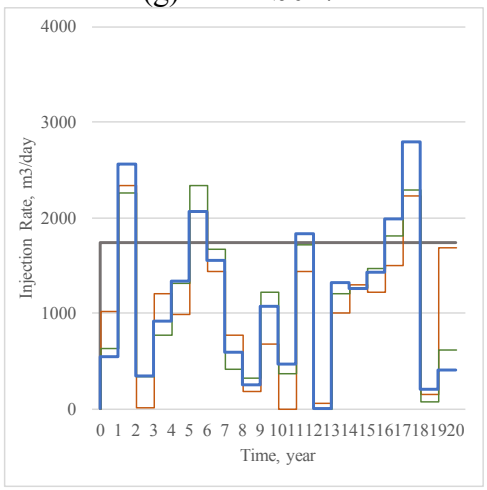

(i) 'INJ021'

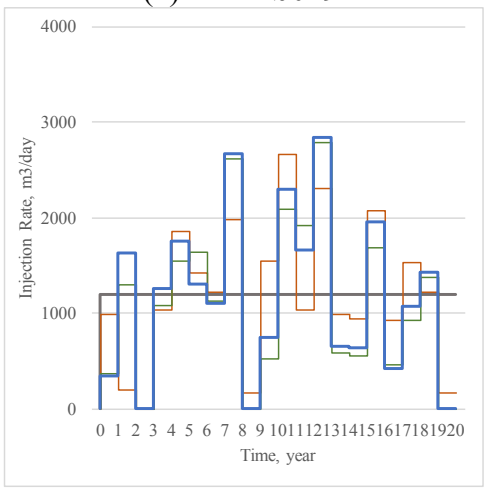

(j) 'INJ022'

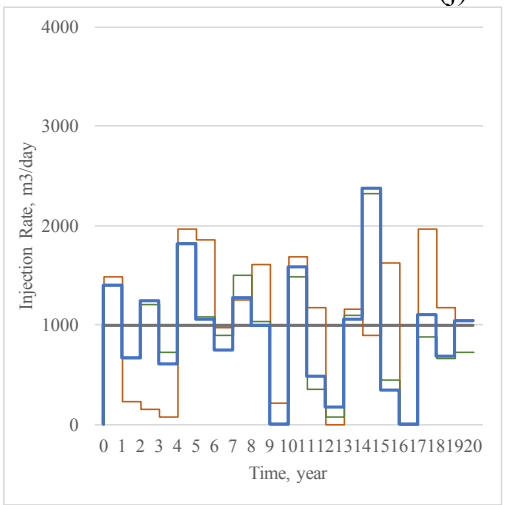

(k) 'INJ023'

Figure 23: Continued.

The EnOpt increases the NPV from $8.07 billion to $8.84 billion, 9.45% increases. The optimization converged in 7 iterations. Figure 24 shows changes of NPV with iterations. The cumulative oil production after optimization slightly increases from 49.58 MM m^3 to 51.65 MM m^3, 4.17% increase (see Figure 25), while the cumulative water production significantly decreases from 62.42 MM m^3 to 43.97 MM m^3, 29.56% decrease (see Figure 26). Unlike the optimal solution from the previous case, the EnOpt's optimal solution increases the NPV by slightly increases the total oil production but significantly decreases in total water production. The saturation maps in Figure 27 show that the EnOpt distributed water more evenly among the injectors. The saturation maps also reflect that the water production is lower in the EnOpt as the water saturation from the EnOpt is lower than the base case.

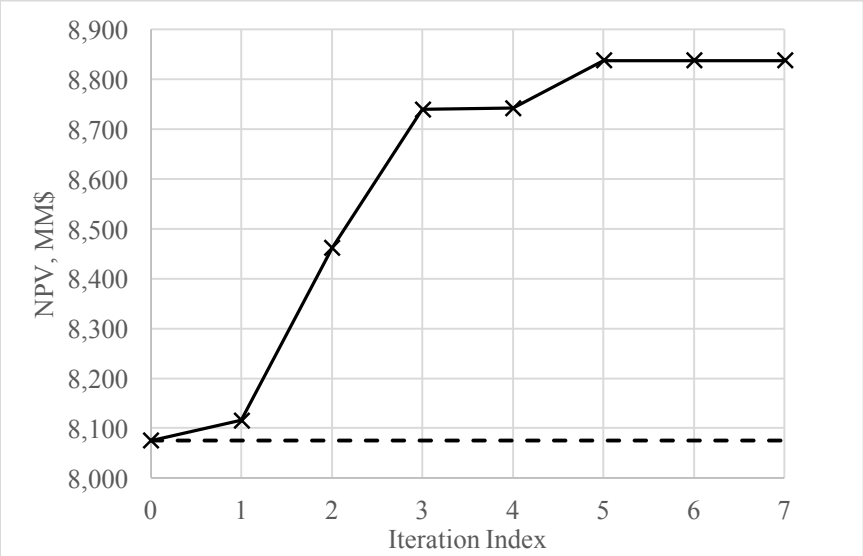

Figure 24: The change of NPV with iterations for the extended production history case. The solid line indicates NPV from EnOpt, the dash line indicates NPV from an equal rate case.

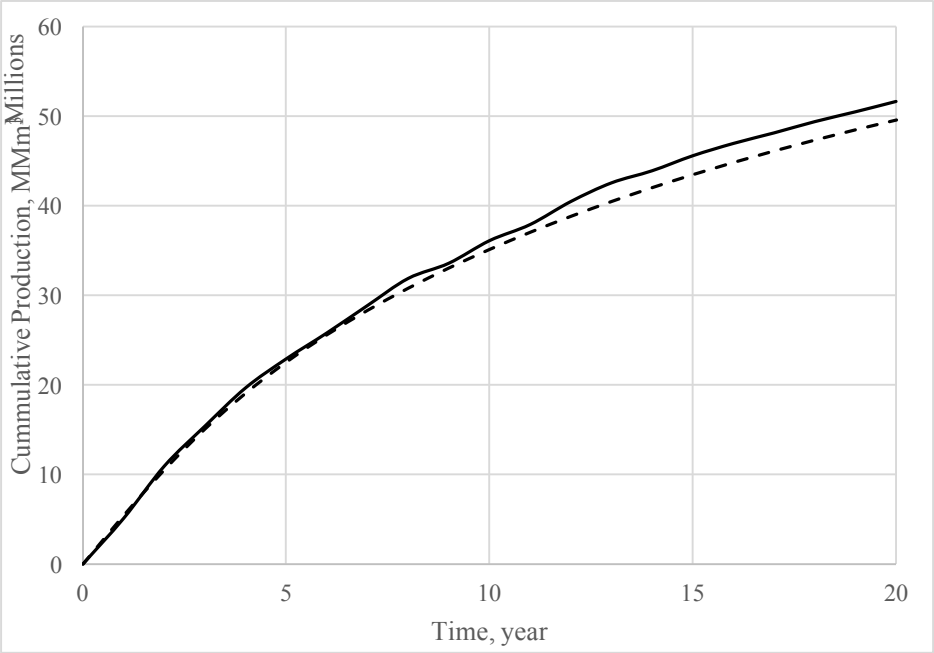

Figure 25: Comparison of cumulative oil production for the extended production history case. The solid line indicates EnOpt result. The dash line indicates base case result.

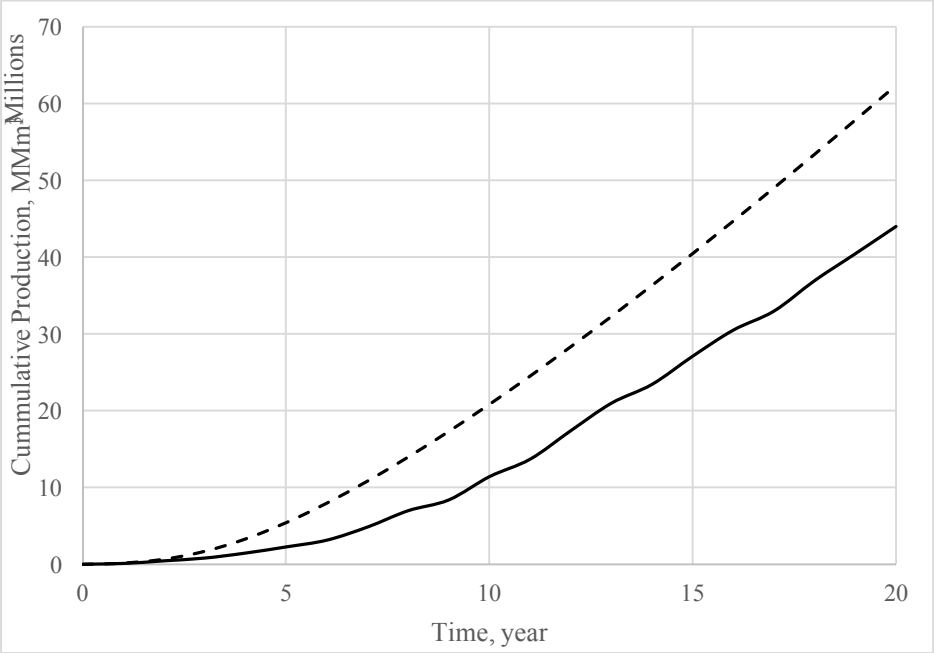

Figure 26: Comparison of cumulative water production for the extended production history case. The solid line indicates EnOpt result. The dash line indicates base case result.

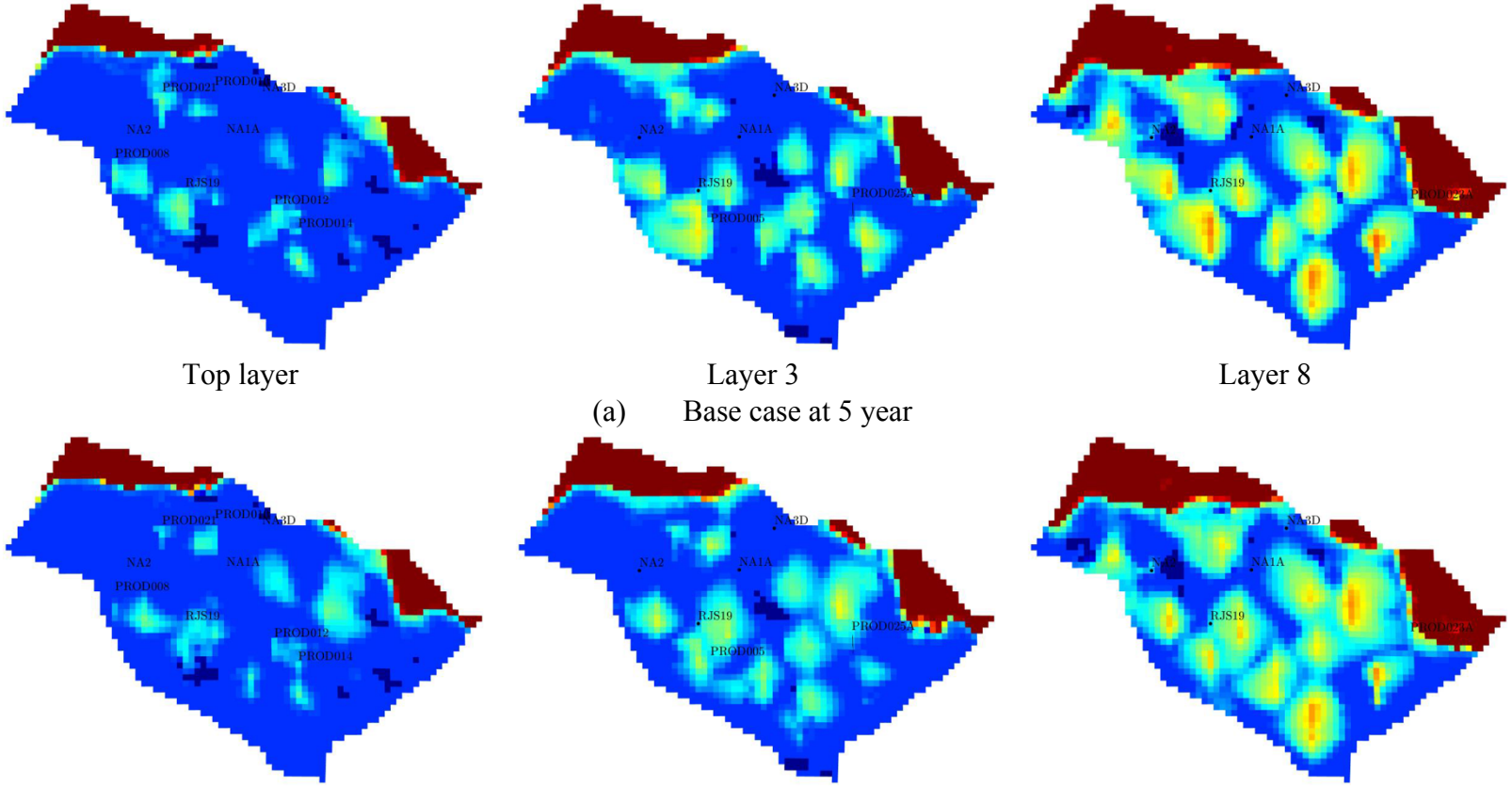

Top layer Layer 3 Layer 8

(a) Base case at 5 year

Top layer Layer 3 Layer 8

(b) EnOpt at 5 year

Figure 27: Saturation maps of some layers at different production time.

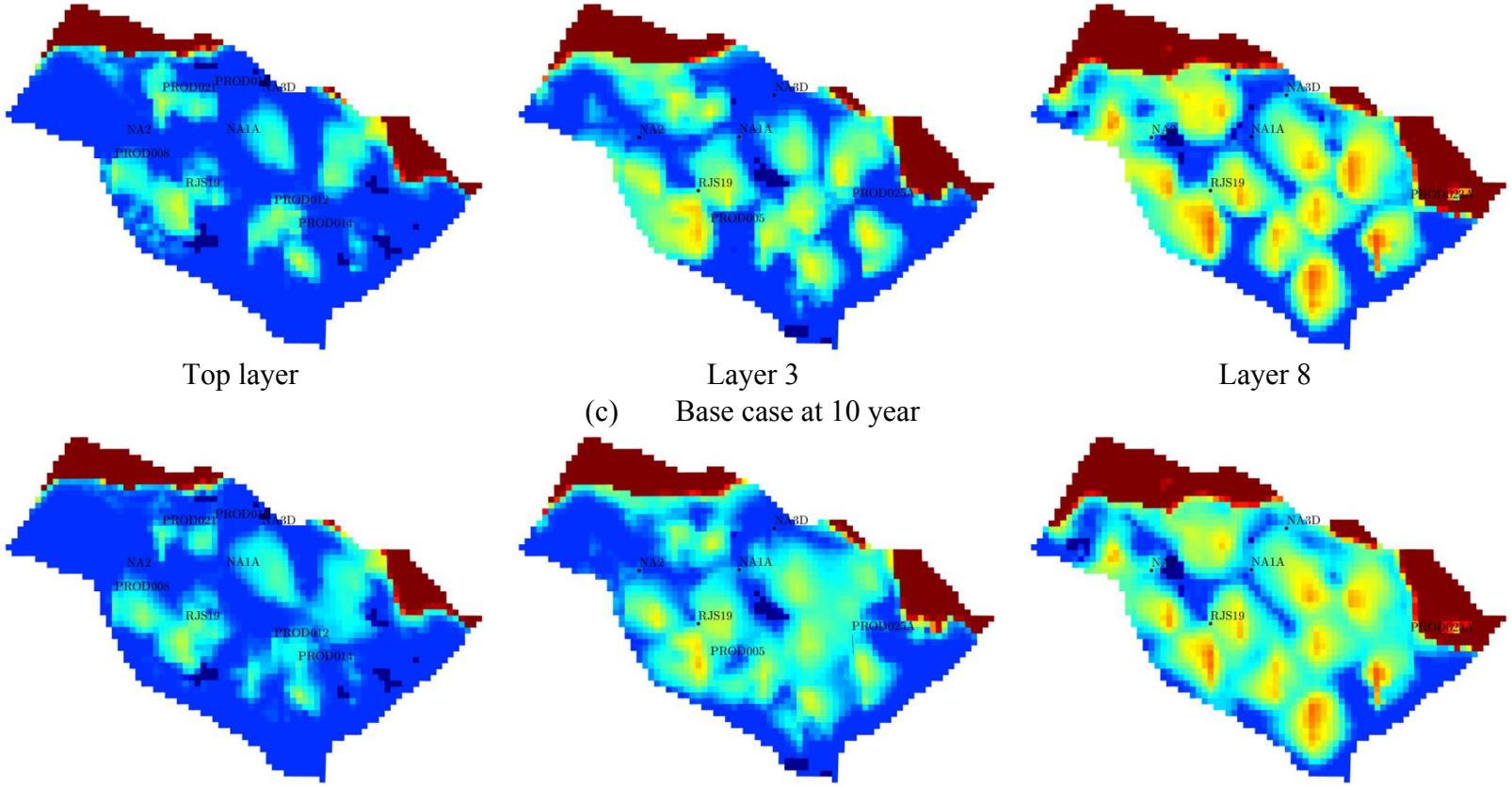

Top layer Layer 3 Layer 8

(c) Base case at 10 year

Top layer Layer 3 Layer 8

(d) EnOpt at 10 year

Figure 27: Continued.

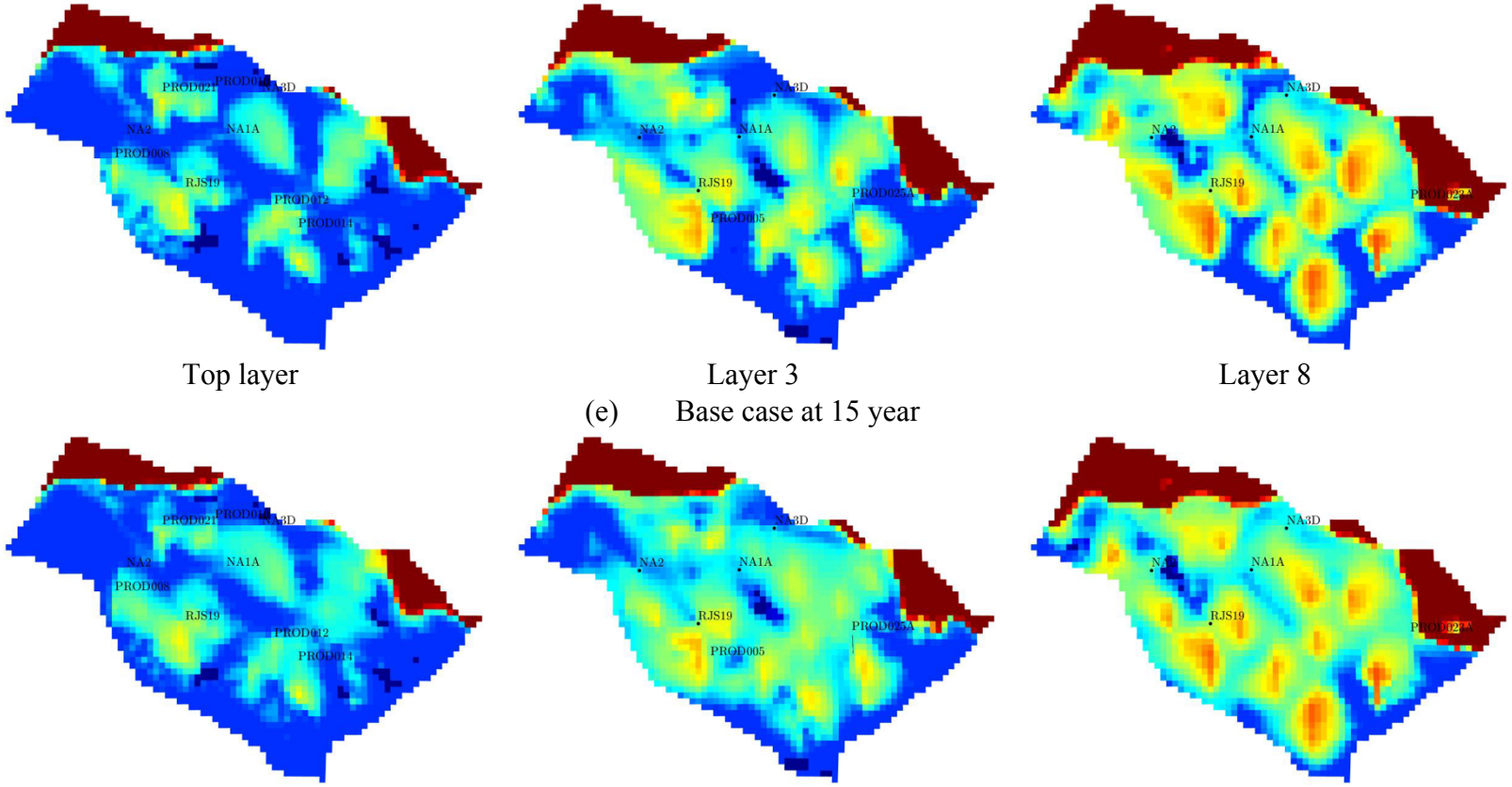

Top layer Layer 3 Layer 8

(e) Base case at 15 year

Top layer Layer 3 Layer 8

(f) EnOpt at 15 year

Figure 27: Continued.

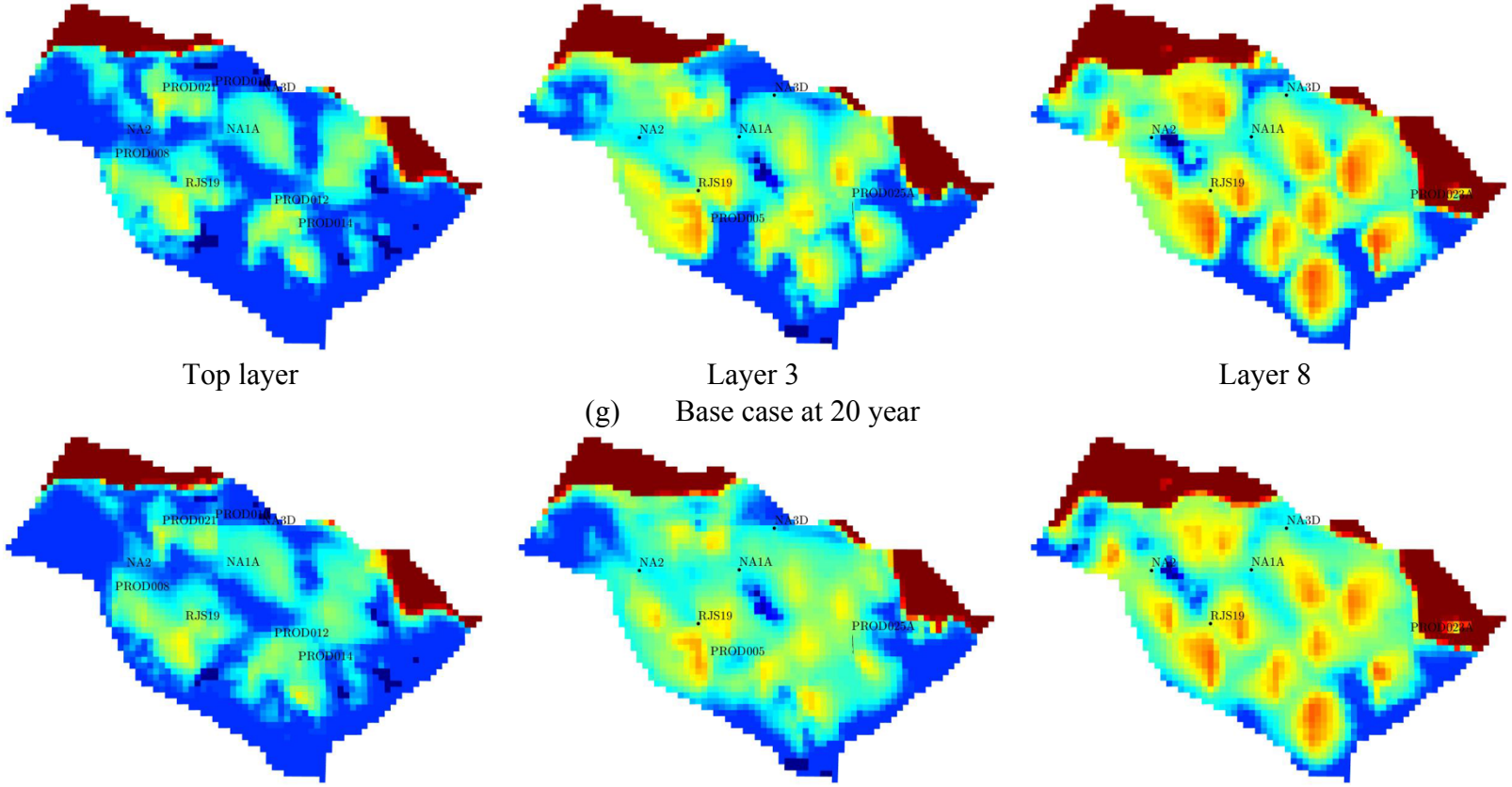

Top layer Layer 3 Layer 8

(g) Base case at 20 year

Top layer Layer 3 Layer 8

(h) EnOpt at 20 year

Figure 27: Continued.

4.4 Long-term and Short-term Production Optimization

A study on the effect of a discount rate r_τ , as in (38), to the cumulative cash flow is discussed in this section. The discount rate is usually used as a tuning parameter when considering interest rate in the computation of NPV as an objective function. The case where highly-discounted NPV is used as an objective function can be referred as a *short-term* optimization. The computation of cash flow weights on early production periods more than later periods. If an undiscounted NPV is used as an objective function, the optimization can be referred as a *long-term* optimization. In this case, cash flow is equally weighted throughout the production time. Although we could apply both optimization schemes into the same reservoir, the goal of each scheme aims to maximize the cash flow in different time frame. The short-term optimization is usually used in the case when we want to increase a cash flow in the near-future time. The long-term, on the other hand, aims to maximize the overall cumulative cash flow throughout the reservoir life-cycle.

To give a clearer picture, we run two optimizations using different discount rate. The optimized results are compared with the same base case used in random initial control settings case. The first case, a long-term production optimization, the discount rate is set to 0. The second case, a short-term production optimization, the discount rate is set to be high at 60% per year. Figure 28 shows the cumulative cash flow from two optimization cases and a base case. The optimal solution from short-term optimization shows an increase in the cumulative cash flow in early production period. However, as the production time approaches to the end, the long-term optimization yields higher cumulative cash flow. The cumulative oil production plot in Figure 29 show the same

trend as the cumulative cash flow. Figure 30 shows the cumulative water production from both optimized result and the base case. The short-term optimization increases the oil production in early of production time and also allows more water to be produced in the later production time. The water production produced in later production time in short-term optimization decreases the net cash flow in those production time. The long-term optimization, on the other hand, constantly produces oil while keeps the water production low throughout the production time. This results in higher cumulative cash flow. In addition, Figure 31 also indicates that in short-term EnOpt, the reservoir is more saturated with water. As a result, more water is produced from the case.

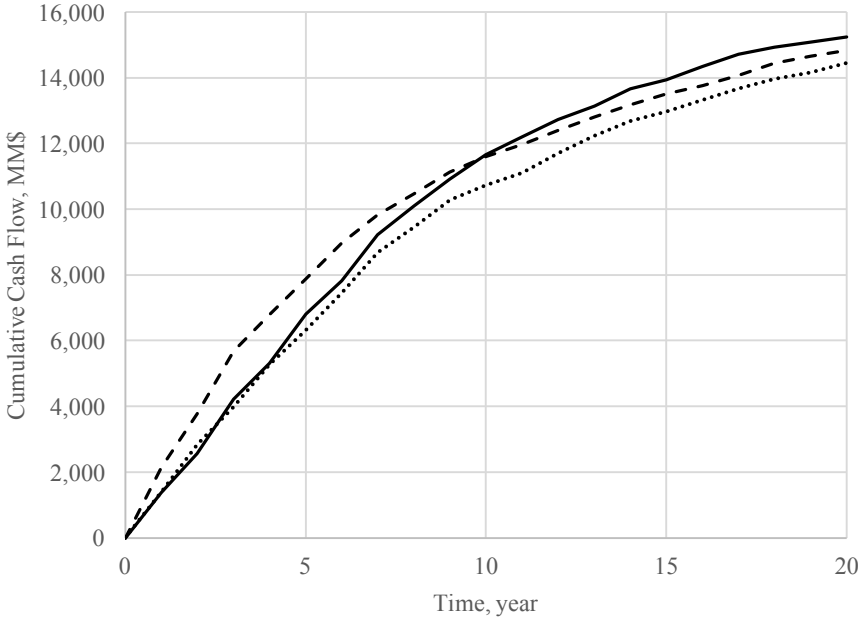

Figure 28: Comparison of cumulative cash flow from long-term, shot-term optimization and the base case. The solid line indicates long-term EnOpt, dash line indicates short-term EnOpt, and the dotted line indicates base case.

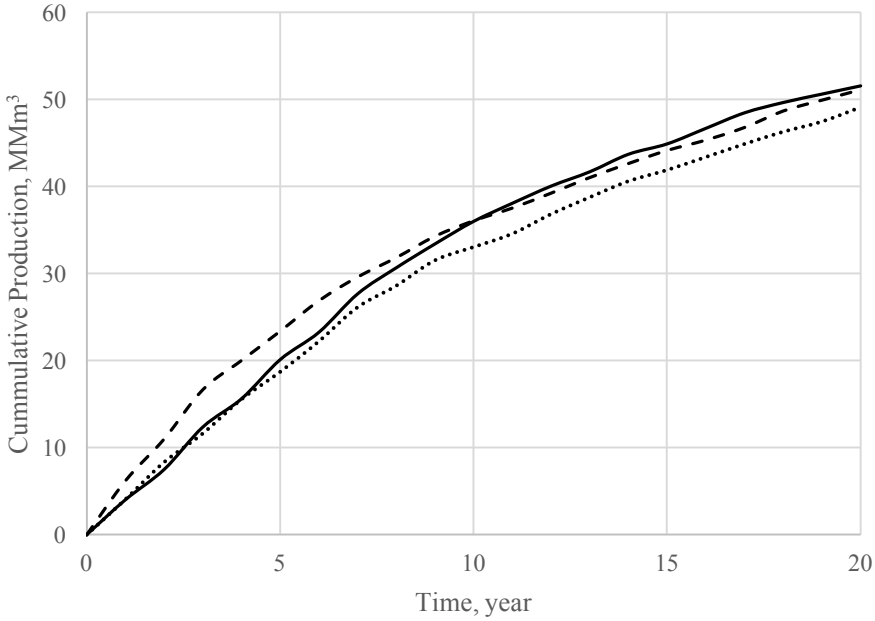

Figure 29: Comparison of cumulative oil production from long-term, shot-term optimization and the base case. The solid line indicates long-term EnOpt, dash line indicates short-term EnOpt, and the dotted line indicates base case.

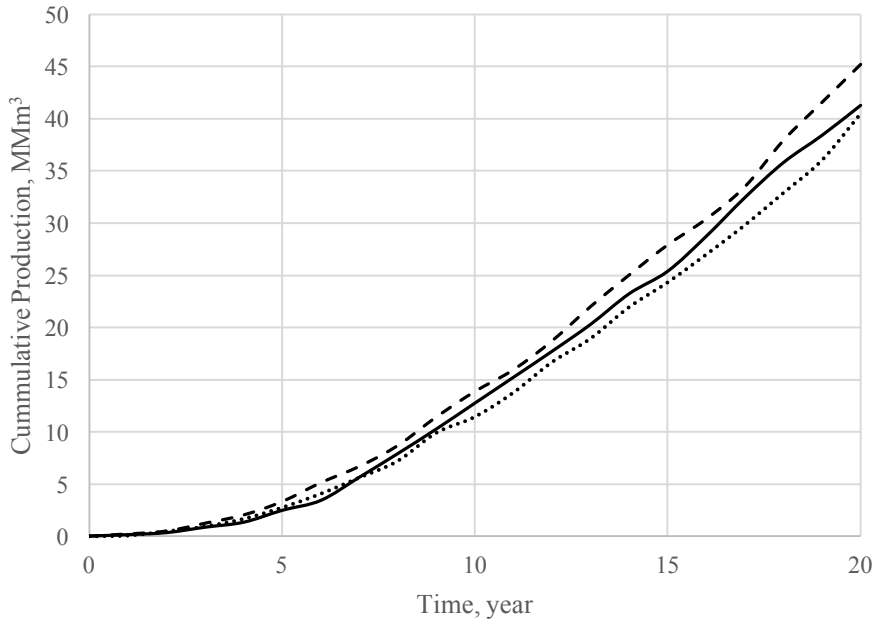

Figure 30: Comparison of cumulative water production from long-term, shot-term optimization and the base case. The solid line indicates long-term EnOpt, dash line indicates short-term EnOpt, and the dotted line indicates base case.

Fonseca et al. (2014) couple short-term and long-term production optimization into a method, so-called, hierarchical multi-objective production optimization. In the method, the long-term NPV serves as a primary objective function while the short-term NPV is used as a secondary objective function. The optimal control from an optimized primary objective function is used as a starting point for an optimization of a secondary objective function. The optimization method increases a cumulative cash flow in early production time while maintaining the life-cycle, or long-term, cumulative cash flow.

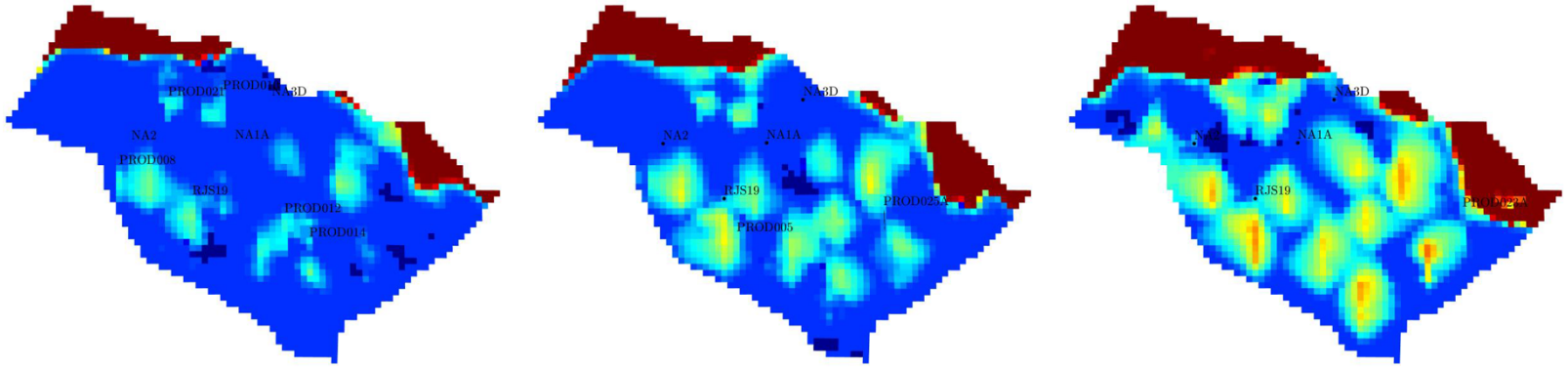

Top layer Layer 3 Layer 8

(a) Short-term Optimization at 5 year

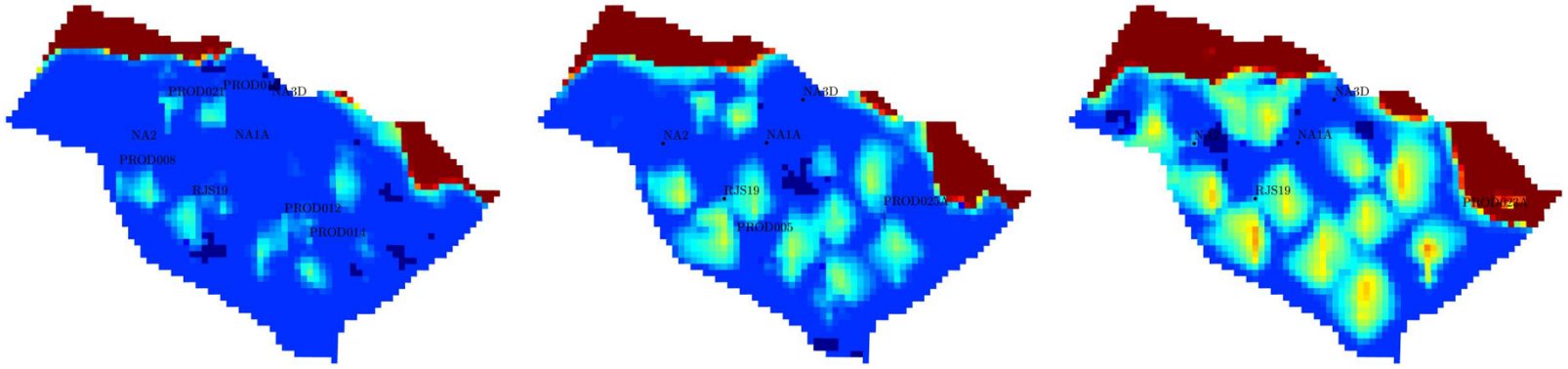

Top layer Layer 3 Layer 8

(b) Long-term Optimization at 5 year

Figure 31: Saturation maps of some layers from short-term and long-term EnOpt at different production time.

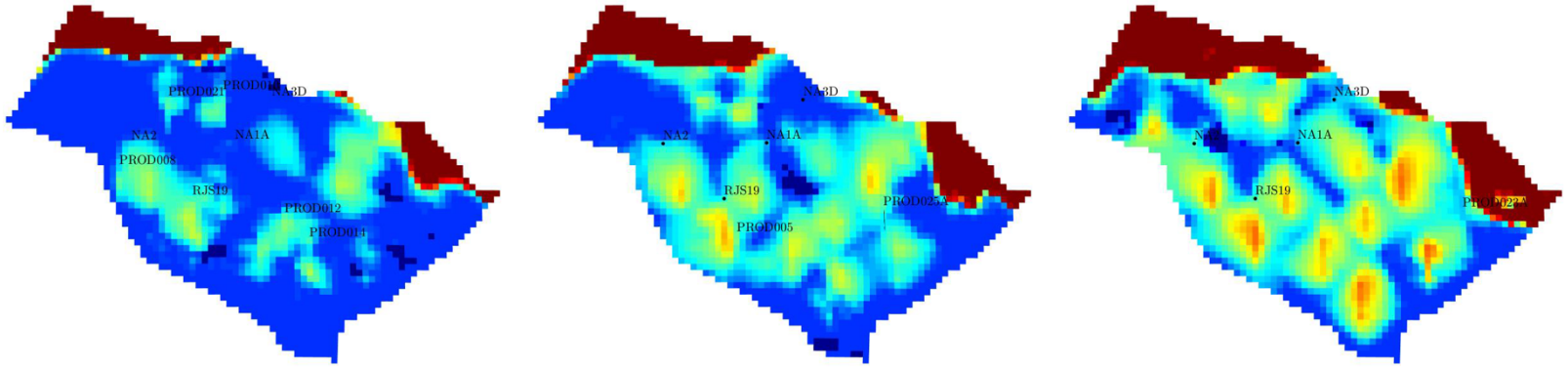

Top layer Layer 3 Layer 8

(c) Short-term Optimization at 10 year

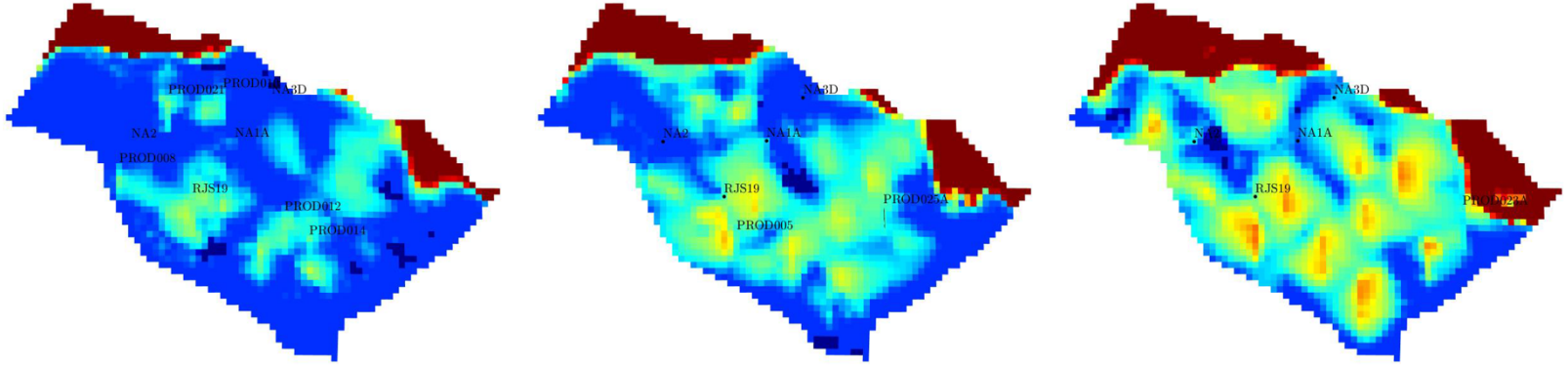

Top layer Layer 3 Layer 8

(d) Long-term Optimization at 10 year

Figure 31: Continued.

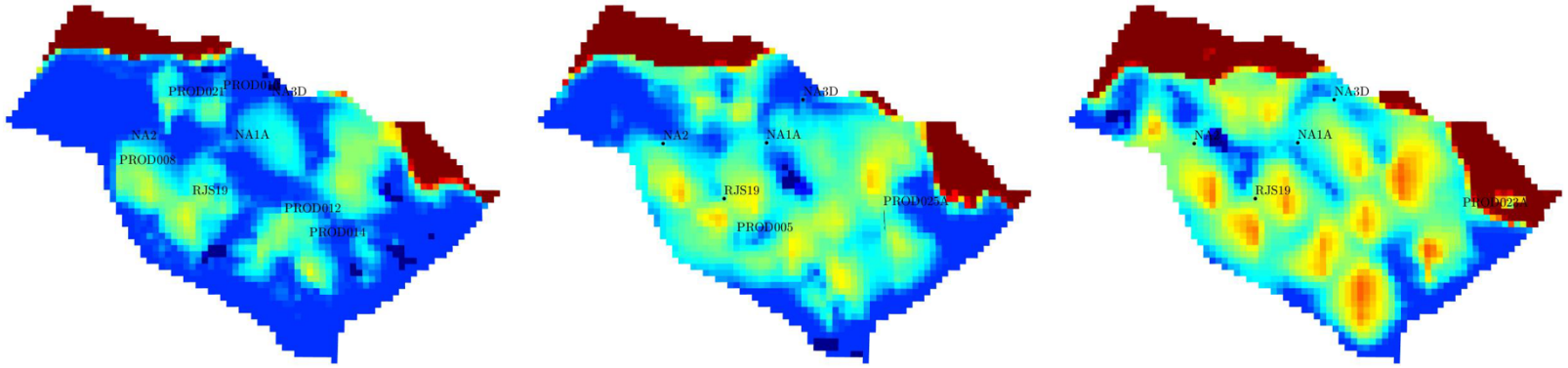

Top layer Layer 3 Layer 8

(e) Short-term Optimization at 15 year

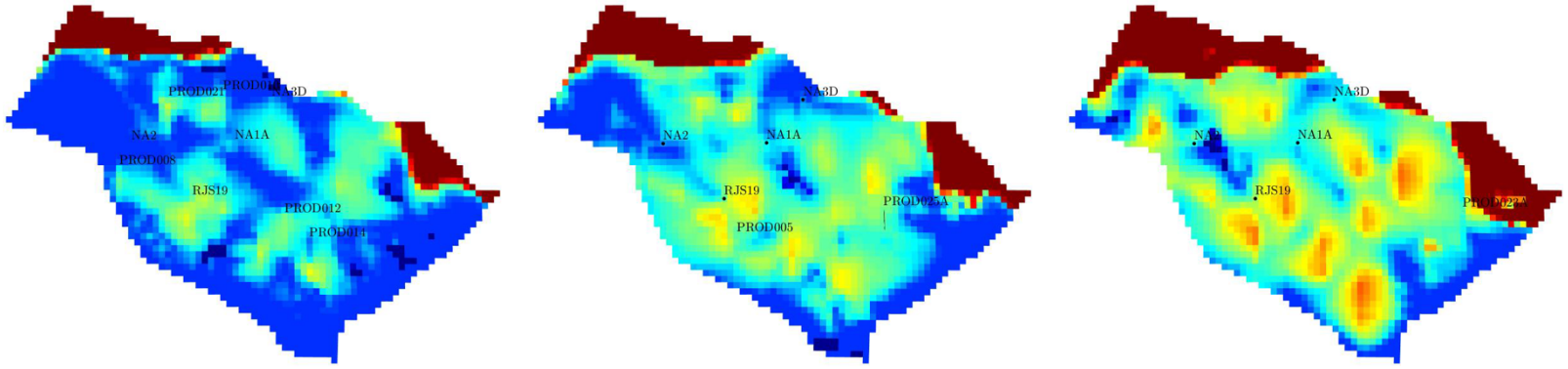

Top layer Layer 3 Layer 8

(f) Long-term Optimization at 15 year

Figure 31: Continued.

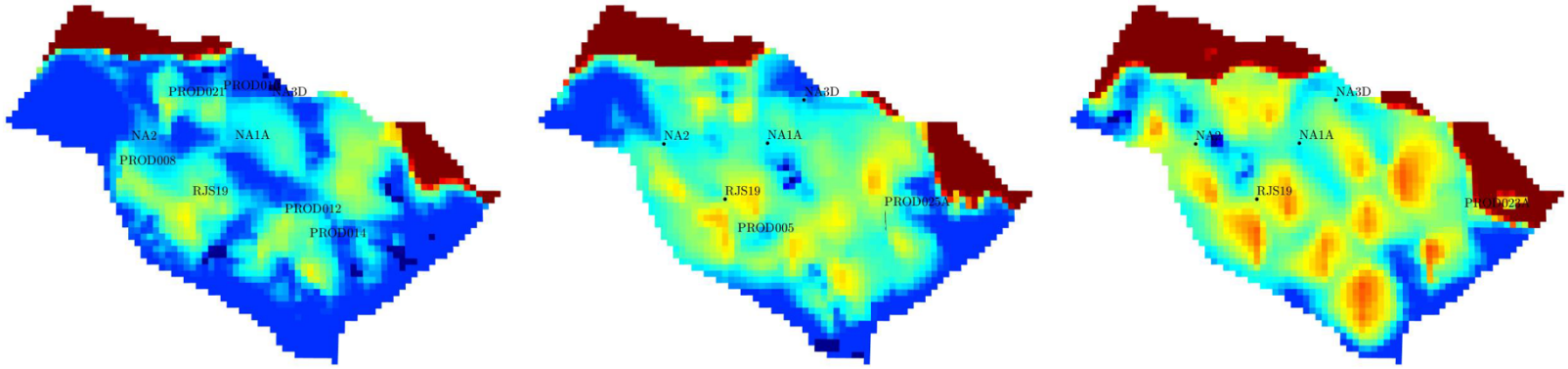

Top layer Layer 3 Layer 8

(g) Short-term Optimization at 20 year

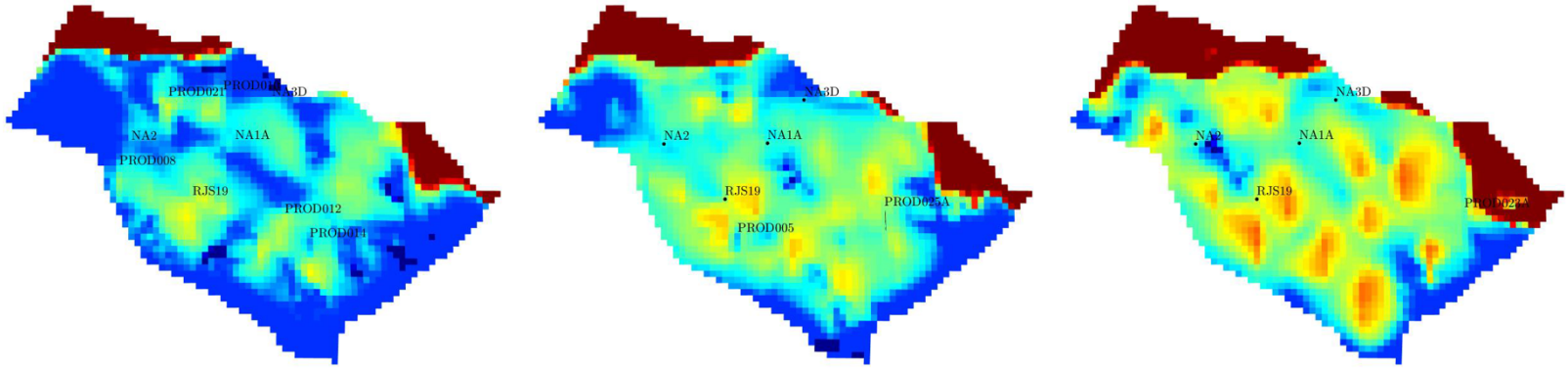

Top layer Layer 3 Layer 8

(h) Long-term Optimization at 20 year

Figure 31: Continued.

5. CONCLUSION

The EnOpt has gained its popularity over the past years in the reservoir simulation community. Many studies have shown that EnOpt has highly potential for future improvement. In this thesis, we have provided some insights of an ensemble-base optimization method (EnOpt) where the optimization is done using steepest ascent method, and the gradient is approximated by an ensemble method. We applied the EnOpt to the synthetic reservoir, namely UNISIM-I. Two optimization cases were performed: random initial control and extended production history. The EnOpt has successfully optimized both optimization cases. In addition, the study about an effect of the discount rate to an optimized solution has also been done. As results of this study, the optimization can be done in two scheme, long-term and short-term optimization. Each optimization scheme aims to maximize the production cash flow in different production time. The long-term optimization aims to maximize the cash flow throughout the lifecycle of the reservoir where the short-term optimization, on the other hand, aims to maximize a cash flow of an early production period. Therefore, the short-term optimization yields higher cumulative cash flow in early production time but the long-term optimization usually results in higher cumulative cash flow at the end of production.

For future improvement regarding the use of the short-term and long-term optimization, they can be coupled together in a method, so-called *ensemble-based hierarchical multi-objective production optimization* (Fonseca et al. 2014). The method has shown an improvement of the cash flow in early production time using short-term

optimization while maintaining the optimized cumulative cash flow at the end of production time from long-term optimization.

Another approach for future study is to implement EnOpt in a close-loop reservoir management. Instead of using a single realization of reservoir model throughout the optimization, in close-loop optimization, the reservoir model is updated continuously once the new geological data is available, enhancing the optimization result to be more accurate.

Lastly, we can improve the EnOpt through a modification of the EnOpt formula. Many recent studies purpose a modified EnOpt formula which demonstrates an improvement of the optimization. The modified EnOpt methods are such as conjugate gradient EnOpt (Chaurdhri et al. 2009), covariance matrix adaptation EnOpt (Fonseca et al. 2013), and Stochastic Simplex Approximate Gradient (Fonseca et al. 2017).

REFERENCES

Avansi, G. D., Schiozer, D. J. 2015. UNISIM-I: Synthetic Model for Reservoir Development and Management Applications. *International Journal of Modeling and Simulation for the Petroleum Industry* **9** (1): 21-30.

Aziz, K., Settari, A. 1979. *Petroleum reservoir simulation*. London: Applied Science Publishers.

Brouwer, D. R., Jansen, J. D. 2004. Dynamic Optimization of Waterflooding With Smart Wells Using Optimal Control Theory. *SPE Journal* **9** (4): 391-402. SPE-78278-PA. http://dx.doi.org/10.2118/78278-PA.

Cauchy, M. A. 1847. M´ethode g´en´erale pour la r´esolution des syst`emes d'´equations simultan´ees. *Comptes rendus hebdomadaires des séances de l'Académie des sciences* **25**: 536–538.

Chaurdhri, M. M., Phale, H. A. et al. 2009. An Improved Approach for Ensemble-Based Production Optimization. Present at SPE Western Regional Meeting, San Jose, CA, 24-26 March. SPE-121305-MS. http://dx.doi.org/10.2118/121305-MS.

Chen, Y. 2008. Ensemble-based closed-loop production optimization. Dissertation, University of Oklahoma, Norman, Oklahoma (2008).

Chen, Y., Oliver, D. S. et al. 2009. Efficient Ensemble-Based Closed-Loop Production Optimization. *SPE Journal* **14** (4): 634-645. SPE-112873-PA. http://dx.doi.org/10.2118/112873-PA.

Chen, Z., Huan, G. et al. 2006. *Computational Methods for Multiphase Flows in Porous Media*. Philadelphia, PA: Society for Industrial and Applied Mathematics.

Conn, A. R., Scheinberg, K. et al. 2009. *Introduction to Derivative-Free Optimization*. Philadelphia, PA: Society for Industrial and Applied Mathematics.

Do, S. T., Reynolds, A. C. 2013. Theoretical connections between optimization algorithms based on an approximate gradient. *Computational Geosciences* **17** (6): 959–973. http://dx.doi.org/10.1007/s10596-013-9368-9.

Ertekin, T., Abou-Kassem, J. H. et al. 2001. *Basic Applied Reservoir Simulation*, Vol. 7. Richardson, TX: Society of Petroleum Engineers.

Fonseca, R. M., Kahrobaei, S. S. et al. 2015. Quantification of the Impact of Ensemble Size on the Quality of an Ensemble Gradient Using Principles of Hypothesis Testing. Present at SPE Reservoir Simulation Symposium, Houston, Texas, 23–25 February. SPE-173236-MS. http://dx.doi.org/10.2118/173236-MS.

Fonseca, R. M., Leeuwenburgh, O. et al. 2013. Improving the Ensemble Optimization Method Through Covariance Matrix Adaptation (CMA-EnOpt). Present at SPE Reservoir Simulation Symposium, The Woodlands, Texas, USA, 18-20 February. SPE-163657-MS. https://doi.org/10.2118/163657-MS.

Fonseca, R. M., Leeuwenburgh, O. et al. 2014. Ensemble-based hierarchical multi-objective production optimization of smart wells. *Computational Geosciences* **18** (3): 449-461. http://dx.doi.org/10.1007/s10596-013-9399-2.

Fonseca, R. R.-M., Chen, B. et al. 2017. A Stochastic Simplex Approximate Gradient (StoSAG) for optimization under uncertainty. *International Journal for Numerical Methods in Engineering* **109** (13): 1756-1776.

Gaspar, A. T. F. S., Avansi, G. D. et al. 2016. UNISIM-I-M: Benchmark Case Proposal for Oil Reservoir Management Decision-Making. Present at SPE Trinidad and Tobago Section Energy Resources Conference, Port of Spain, Trinidad and Tobago, 13-15 June. SPE-180848-MS. http://dx.doi.org/10.2118/180848-MS.

Gaspar, A. T. F. S., Avansi, G. D. et al. 2015. UNISIM-I-D: Benchmark Studies for Oil Field Development and Production Strategy Selection. *International Journal of Modeling and Simulation for the Petroleum Industry* **9** (1): 47-55.

Leeuwenburgh, O., Egberts, P. J. P. et al. 2010. Ensemble Methods for Reservoir Life-Cycle Optimization and Well Placement. Present at SPE/DGS Annual Technical Symposium, Al-Khobar, Saudi Arabia, 4-7 April. SPE-136916-MS. http://dx.doi.org/10.2118/136916-MS.

Lie, K. A. 2016. *An Introduction to Reservoir Simulation Using MATLAB: User guide for the Matlab Reservoir Simulation Toolbox (MRST)*. Oslo, Norway: SINTEF.

Lie, K. A., Krogstad, S. et al. 2012. Open-source MATLAB implementation of consistent discretisations on complex grids. *Computational Geosciences* **16** (2): 297-322. http://dx.doi.org/10.1007/s10596-011-9244-4.

Lorentzen, R. J., Berg, A. et al. 2006. A New Approach For Dynamic Optimization Of Water Flooding Problems. Present at Intelligent Energy Conference and Exhibition, Amsterdam, The Netherlands, 11-13 April. SPE-99690-MS. https://doi.org/10.2118/99690-MS.

Meza, J. C. 2010. Steepest descent. *Wiley Interdisciplinary Reviews: Computational Statistics* **2** (6): 719-722. http://dx.doi.org/10.1002/wics.117.

Nocedal, J., Wright, S. J. 2006. *Numerical Optimization*, 2nd edition. New York: Springer.

Sarma, P., Aziz, K. et al. 2005. Implementation of Adjoint Solution for Optimal Control of Smart Wells. Present at SPE Reservoir Simulation Symposium, Woodlands, Texas, 31 January-2 Feburary. SPE-92864-MS. http://dx.doi.org/10.2118/92864-MS.

Stordal, A. S., Szklarz, S. P. et al. 2016. A Theoretical look at Ensemble-Based Optimization in Reservoir Management. *Mathematical Geosciences* **48** (4): 399-417. http://dx.doi.org/10.1007/s11004-015-9598-6.

Wang, C., Li, G. et al. 2007. Production Optimization in Closed-Loop Reservoir Management. Present at SPE Annual Technical Conference and Exhibition, Anaheim, California, 11-14 November. SPE-109805-MS. http://dx.doi.org/10.2118/109805-MS.